Underwater Wireless Power Transfer Modelling and Simulation

(Study on Foreign Metal Objects)

Aidana Toibekkyzy

Submitted in fulfillment of the requirements for the degree of Master of Science in Electrical and Computer Engineering

School of Engineering and Digital Sciences Department of Electrical and Computer Engineering Nazarbayev University

53 Kabanbay Batyr Avenue, Astana, Kazakhstan, 010000

Supervisor: Mehdi Bagheri

Co-supervisor: Annie NG

5 April 2024

Abstract

For a long time, the Autonomous Underwater Vehicle (AUV) has played a vital role in deepsea investigations and the exploration of ocean resources. However, the primary concern related to underwater vehicles is the lack of sufficient battery capacity to sustain their numerous high-power sensors and their durable autonomous activities under the sea. In comparison with the traditional methods of powering AUVs, the Wireless Power Transfer (WPT) systems ensure the transfer of electricity without any usage of cables or wires. It ensures a prolonged mission duration and mobility of AUV, increasing its performance. Eliminating the plugging-in and -out procedures, the WPT technology provides a safe and practical solution for powering AUVs. However, there are a number of factors of the seawater medium that cannot be manually controlled. Such considerations make it complex to model a system able to transfer power with adequate efficiency. Therefore, this thesis analyzes an underwater WPT system and investigates its behavior under different conditions of the surrounding environment. It provides a quantitative analysis of the influence of the environment, external objects, and misalignment between the resonators on the electrical properties of the coil and the performance of the underwater WPT system. This is performed by testing the WPT in different media, namely in air, seawater, and more conductive water; testing in the presence of objects with different material types, sizes, thicknesses, and shapes; as well as testing the model when coils are not perfectly aligned. The results suggest that the conductive environment causes more eddy current generation, decreasing the efficiency of WPT. The placement of foreign objects differently affects the system, depending on the induced eddy currents on them, the magnetization effect, and how localized the magnetic field is around the coil.

Table of Contents

List of Abbreviations and Symbols

AUV	Autonomous Underwater Vehicle
CPT	Capacitive Wireless Power Transfer
DC	Direct current
IPT	Inductive Wireless Power Transfer
P-P	Parallel-Parallel compensation topology
P-S	Parallel-Series compensation topology
PTE	Power transfer efficiency
RF	Radio frequency
Rx	Receiver
S-S	Series-Series compensation topology
S-P	Series-Parallel compensation topology
Tx	Transmitter
UWPT	Underwater Wireless Power Transfer
WPT	Wireless Power Transfer

List of Figures

List of Tables

Chapter 1 - Introduction

1.1 - Background

The growing demand for the exploration of ocean resources has led to the development of subsea devices capable of gaining access to and exploiting them. Autonomous Underwater Vehicle (AUV) plays a vital role in such deepsea investigations since it has precise maneuvering and is not limited by umbilical cables. These submersible robots have no requirement for being connected to the support vessel and, therefore, contain onboard navigation and energy storage systems [1]. Such board equipment results in independent travel for the prolonged period of time throughout the ocean. AUVs are extensively employed in commercial applications namely subsea surveys, underwater mining, and off-shore oil drilling [2], [3]. There is also a growing interest in other applications such as surveillance, mapping, delivery, search and rescue [4].

Ocean exploration is a massive activity and requires from several hours to several days. Therefore, to ensure the successful mission completion of AUVs, the amount of time for their autonomous operation should be guaranteed to be as long as necessary [5]. However, the primary technical challenge related to underwater vehicles is the lack of sufficient battery capacity to sustain its numerous high-power sensors and its durable autonomous activities under the sea [2-6]. There are two common techniques for powering up underwater vehicles [3]. One of them includes pulling the vehicle out of the water and recharging it or replacing the battery. Such a method needs a mother ship platform located close enough for serving the technical support. Another charging method involves physically connecting cables while an AUV is still in the sea environment. This substantially reduces the autonomy and performance of the submersible vehicles [3] due to the restrictions by installed cables. Apart from that, both techniques are in need of human intervention

and do not comply with the ocean surveillance systems' self-service criteria. Therefore, AUVs demand an alternative method of its charging.

This thesis proposes a viable solution for the AUV's extended and successful use that addresses the mentioned issues and contributes to its charging gaps. The existing literature review demonstrates that the wireless charging of these devices makes AUVs more durable than conventional charging. Underwater wireless power transfer (UWPT) technology exhibits a practical and safe energy transmission solution for AUVs [1]-[3]. These systems ensure the transfer of the electricity from the charging source straight to the AUV without any usage of cables or wires. Such a mechanism does not limit the movement of the vehicle but rather increases its mobility. This, in turn, enhances the performance of the AUV. Apart from that, due to the absence of cable and plug-and-socket connections undersea, the wireless charging system eliminates the spark dangers during plugging-in and plugging-out operations [3]. It also prevents the corrosion that occurs because of saltwater exposure. Thereby, the UWPT provides non-dangerous functioning to the AUVs.

Integrating an UWPT system into an AUV board might be challenging since its hull structure is composed of materials (mostly aluminum and titanium) that are highly conductive. The researchers in [7] reported on an AUV equipped with an aluminum hull that housed its secondary coil. This led to an obvious decrease in power transfer efficiency compared to when no such structure existed. Similarly, previous designs such as those described in [3], [8], and [9] involved altering the AUV structure by adding projections outside its hull for a docking mechanism made of aluminum. As a result, the UWPT system geometry has to be altered appropriately so the performance of power transfer would not be affected significantly. In this regard, the design described by [10] uses arc shaped magnetic couplers with a receiver coil positioned directly on the

AUV's curved hull. This method provided a generation of higher magnetic flux density within the couplers, which in turn, increased the system's efficiency.

Despite that, the mentioned alternative of changing the UWPT system geometry may not always keep the desired performance of the system when external objects are positioned between the receiver and transmitter coils. Since these objects interfere with the magnetic field that is produced by the coil, they have a considerable impact on the inductive power transfer. On this behalf, the influence of the external object on the Class-E inverter in the WPT system is analyzed in [11]. Similarly, the effect of the metal object on the loosely coupled WPT system is investigated in [12]. However, both studies consider only a few changing variables, such as the location of the obstacle. The vast majority of work has been done on Foreign Object Detection techniques as in [13-15], the latter which implements a sensor coil winded on the transmitter. These studies mainly focus on the thermal heating by the strong magnetic field due to the foreign object and/or a drop in the system's efficiency. Hence, the studies regarding the inductively coupled WPT systems for underwater applications, particularly in the presence of external object cases, still remain concerning.

Along with the listed issues, there are specific gaps related to the underwater WPT systems due to the increased losses in seawater. Such an environment is capable of blocking electromagnetic waves with high frequencies. Hence, the resonant frequency choice should be made properly when designing the wireless charging system for underwater use. It is imperative to note that the water properties should be considered in the theoretical analysis, which is generally neglected in the study of conventional WPT systems. The existing literature on underwater WPT systems also does not take the properties of the natural seawater into account: the majority of the research has been done on testing a WPT in freshwater. However, seawater is known to be saltier, and the salinity (meaning conductivity) ranges from $4\,S/m$ to $6\,S/m$. Furthermore, seawater, in real cases, is often not

stationary. Generally, due to the natural flow or due to other disturbance factors (i.e., the flowing ship's interaction with the surrounding water), the water in the sea becomes turbulent. Hence, the perfect alignment of the receiver and transmitter coils is not guaranteed in such scenarios. Moreover, the application of the WPT system into the real world considers the disturbances on the couplers from the surrounding environment, as was discussed earlier. Such obstacles can appear in the form of any object made of any material and cause a degradation of power transfer efficiency. It can be observed from Figure 1.1 that the presence of any metal object in the working volume of WPT considerably affects the electromagnetic field and generates eddy currents [16]. Nonetheless, the WPT system has to continue working and perform desirably even in those situations.

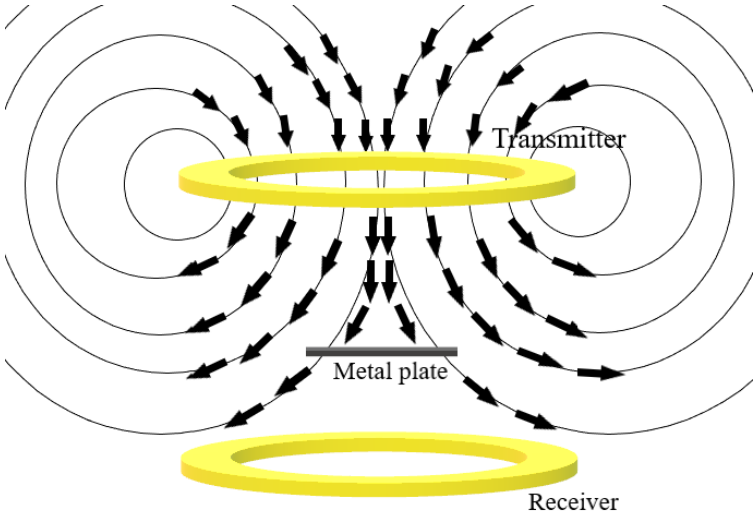

Figure 1.1: The magnetic field density distribution in the presence of metal object

These considerations make it complex to model a system able to transfer the power with adequate efficiency (preferably above 50%). Therefore, overcoming these challenges and implementing the real-case scenarios to test the performance of underwater WPT systems can open up new possibilities. It will ensure that the operational and mission duration ranges are increased and are not interrupted due to surrounding obstacles.

1.3 - Objectives

The objective of this thesis is to analyze an underwater WPT system and investigate its behavior under different conditions of the surrounding environment. The first scenario includes testing the system efficiency in air, seawater, and more conductive water to study the relationship between the performance of the WPT system and the electromagnetic properties of three different media can be obtained. The parameters of the environment influence the efficiency of wireless charging technology. Therefore, this knowledge is significant for implementing WPT in underwater applications.

During the second scenario, one of the couplers of the WPT system is shifted from its original position to study the relationship between the coupling coefficient of IPT and lateral misalignment. Here, the coupling coefficient reflects the effectiveness of WPT. Hence, by examining this scenario, the vulnerability of the underwater IPT system to the misaligned coils can be investigated. This can lead to the development of new techniques that provide the desired performance of the system even when coils are not perfectly aligned.

The third scenario investigates the performance of the underwater IWPT system in the presence of external objects. The samples of the tests are the circular and rectangular plates. The latter is studied in different sizes, thicknesses, type of material and positioning. These objects are located between two couplers. The purpose of these tests is to mirror the real-world situations that reflect how the system might perform in such cases. The key metrics of this study are power transfer efficiency, mutual inductance and mutual resistance.

The fourth scenario considers the placement of the ‘aluminum can’ between the couplers. This demonstrates how the commonly found object in a water environment can interact with the IPT system and affect it. The ‘aluminum can’ is positioned in three different locations to imitate its

movement in water. Therefore, the influence of dynamic environmental factors on the underwater IPT system is also in the scope of this work.

1.4 - Thesis organization

This report includes 6 chapters. The background information related to the topic of this study, its scope and significance are presented in Chapter 1. The research problem related to AUV's charging

Chapter 2 reviews the WPT system categories and technologies with a discussion of the benefits and disadvantages of each. It then analyzes the fundamental theory of inductive coupling and mutual inductance. After that, this section provides the state-of-the-art for each technology.

Chapter 3 analyzes and presents the fundamental principles necessary for understanding this work. It starts with the inductive coupling model theory, followed by mutual inductance. It then describes the compensation network technologies, along with the water qualities, since they have a significant influence on the energy transmission of WPT.

Chapter 4 presents the coil design and model of the proposed inductive WPT system. The section explains how the simulations are conducted, the four scenarios used for testing the system, as well as the sample choice used in two of the scenarios.

In Chapter 5, the results of the conducted simulations are demonstrated. Outcomes of each relevant scenario are compared with each other through the graphic representation. Then, the detailed discussion on these outputs are provided.

Chapter 6 concludes this thesis by outlining the work performed. The limitations, as well as recommendations for future work on underwater WPT system study, are also presented.

Chapter 2 - Literature Review

A Wireless Power Transfer (WPT) system provides power movement without any usage of physical wires. The concept of this technology dates back to Nikola Tesla in 1912 when he suggested this form of electrical distribution via the air [6]. The WPT systems are classified into two types namely radiative and non-radiative. The classification depends on how energy is transmitted, meaning each has unique applications [2], [6], [17].

The radiative WPT system applies microwave or laser beam technology for power transfer from one point to another. This system is also known as far-field WPT since it ensures that the energy is transmitted over long distances up to several meters. The operational range includes high frequencies, between 300 MHz - 300 GHz [2], [9]. An American engineer William C. Brown first presented this idea during the 1960s. He claimed that microwave energy can be used for energy transmission and demonstrated an aircraft that was successfully powered wirelessly via a microwave beam [2]. A radiative WPT system includes both an energy-radiating resonator (an antenna) and a rectenna, which converts AC power into DC energy. Although efforts have been made to implement radiative WPT systems for underwater use without success so far - with attenuation-induced medium losses serving as their main drawback [18], [19]. Water has particular properties that influence the electromagnetic waves. The absorption and scattering processes also affect them, especially those waves in microwave and radio frequency (RF) bands. Such phenomena considerably decrease the power transfer efficiency. Moreover, marine life can be exposed to these electromagnetic waves, which puts an ecosystem underwater in high danger. Therefore, the impact caused by seawater and radiative risks makes radio waves unsuitable for their use underwater.

The nonradiative WPT system, on the other hand, utilizes an electromagnetic induction principle for energy transmission through the magnetic fields. These magnetic fields are not

radiative, indicating that the power resides within a small area of the transmitter. If the receiver is located within this area, the power transmission occurs otherwise no energy is transmitted. Therefore, the energy transfer range of nonradiative wireless systems is within short distances and is dependent on the dimensions and geometry of the resonators [20]. This ensures that the coupling is strong between the transmitting and receiving sides. On this behalf, the nonradiative WPT systems are usually referred to as near-field technology [6]. The capacitive and inductive wireless power transfer (CPT and IPT) techniques represent the nonradiative WPT systems [20].

2.1 - Capacitive Wireless Power Transfer

The CPT systems consist of two metal plates and use electric fields with high frequencies to deliver energy [6], [7]. These capacitive systems have multivarious advantages, namely the capability of transmitting power in kilowatt ranges, lower eddy current losses [17], and high tolerance to lateral misalignment [19]. Apart from that, CPT suggests cost-effectiveness due to utilizing metal plates [9]. It is compact [21], allowing the board to equip more required components. However, there is a lack of studies done on the CPT systems. It is imperative to note that in powering up the vehicle, these technologies have only recently been implemented.

In view of this, the prototype of such a capacitive wireless power transmission system that aims the application in freshwater is reported in [22]. The study in [23] proposed a four-plate CPT system that aimed and succeeded in energy transmission in a salty water environment when maintaining lower resonance voltage. Another study [24] explored the use of underwater CPT technology for powering up electric ships. It demonstrates how this type of WPT can generate a power up to megawatts. This amount of electricity is sufficient for quickly powering an electric ship. However, the operational distance of the CPT system is usually limited (up to millimeters). Moreover,

applying high voltage to the electrodes can cause potential risks which can affect the system's work. Therefore, the capacitive power transmission technology has only been applied for low-power devices of four-plate [25].

2.2 - Inductive Wireless Power Transfer

The inductive WPTs (IWPT) is another technique related to near-field wireless charging technology. It employs a near-field magnetic coupling for power transmission between two resonators [6]. The inductive power transmission systems work based on Faraday's and Ampere's Laws. The Ampere's Law states that a magnetic field is generated around a transmitting coil that carries a time-varying current. This field is proportional to the current's magnitude. The constant of this proportionality relationship is equal to the permeability of a free space [26]. When a time-varying magnetic field interacts with the receiving coil at its terminal, an alternating electromotive force (emf) is generated according to Faraday's Law [27], which induces an alternating current to flow through a receiver. In combination, the Faraday's and Ampere's Laws contribute to the principle of IWPT.

The IWPT systems had been commonly used for charging devices like smartphones, electric toothbrushes, laptop computers, and tablets [1], [20]. Despite that over the past decade, inductive wireless charging technology has rapidly advanced. Today it provides well-established solutions for charging electric vehicles that require power ranging from microwatts up to several hundreds of kilowatts [28]. Current inductive WPT systems for underwater vehicles tend to boost power output in the kilowatt range that produces less than 10% losses [22]. Heeres et al. [23], in 1994, first presented the concept of an inductive power transfer system for submerged devices when they developed their 3-kVA model to supply energy from surface ships or buoys directly to submerged

loads. The proposed system adopts a linear coaxial winding transformer as its coupler design. Feezor et al. [24] presented another underwater IWPT solution using a 200-W interface transformer in 2001 for their Odyssey IIb AUV solution. In order to provide design guidelines for underwater IPT, the influence of eddy current loss on its performance was investigated in [25] and [29].

Research into underwater IPTs not only addresses AUV charging needs but also attempts to improve misalignment tolerance. In this regard, the WPT system in [30] implemented a rotation-resilient coil structure which consisted of a receiver with two cores and three transmitters. Such structure contributed to relatively continuous power transmission at misalignment and obtained 86.19% of efficiency at perfect alignment. Another study [31] adopted two decoupled receiver coils whose magnetic flux directions are normal to each other. This approach maintained almost constant mutual inductances at rotational misalignment. The system achieved stable efficiency values of 92.26% in the best case-and 92.10% in the worst-case scenario. Yan et al. [32] designed a lateral misalignment-tolerant underwater WPT system using two circular planar coils. The system's efficiency remained stable between 215.5 kHz and 248.4 kHz in air and water environments. The study also provides an analysis of the change in eddy current losses under misalignment at different resonant frequencies.

Changing the coil geometry of IPT, in turn, can address poor performance of the underwater WPT system by enhancing its efficiency since coil parameters have a significant influence on the mutual inductance and coupling coefficient. On this behalf, researchers in [26] presented cone-shaped coils for powering AUVs. The system was able to transmit power with 93.1% efficiency at a transfer range of 48 mm and performed well underwater fluctuation. The authors claim that more efficiency could be achieved by increasing the size of the coils. Another attractive coil design is proposed in [33], where authors implemented curly coils embedded in the hull of an AUV. Due to

hull compatibility, this coil design does not restrict the receiver size with a radius of 150 mm. The system achieves a power delivery at 95% efficiency, indicating that the curly shape has a potential for underwater use. However, the weight of the receiver coil increases with the rise in dimension, leading to the heavy weight of the AUV. This results in reduced maneuverability and increased consumption of energy, which are undesirable.

Since IPT also works at high frequencies, additional components are incorporated into the system in order to achieve a resonance. This enables to lower the operational frequency of WPT and reduce the coils' size. Such a way of improvement of IPT is also known as compensation. There are different types of compensation networks, each having a particular superiority. A comprehensive analysis of three compensation systems is discussed in [34]. Researchers concluded that the LCC-S type system is not significantly affected by the frequency change since it highly resists fluctuations due to changes in the coupling coefficient. Despite this, the S-S topology is preferable since it exhibits an optimal power transfer efficiency. On this matter, the design of the wireless charging system with S-S topology for underwater applications is presented in [35]. The system obtains 90% efficiency under the angle shift at the receiver resonator, with a fluctuating rate of 2.5%. It indicates that S-S topology is a good candidate for the UWPT system.

Apart from compensation, using several receivers and transmitters, meaning additional resonators, can substantially enhance the power transmission efficiency. This method is known as the domino WPT system. Placing additional resonators increases the transmission distance and high energy transfer capability [36]. The same technique was utilized in [37], where the design of a domino WPT system for unmanned aerial vehicles (UAVs) and a shielding layer was proposed. The number of repeaters, as well as their location variable, was identified by using an optimization algorithm. This enables a reasonable power transfer of 58% at a prolonged distance of 58.4 cm.

Another study [17] reported a resonant domino IPT system with four resonator coils. The proposed design operates at 18.5 kHz and achieves a power transmission with an efficiency of 65% at a distance of 15 cm. Despite all the advantages of improving the transfer distance by placing several repeaters, the domino WPT system for underwater use has yet to be extensively investigated as no literature exists on this [38].

Table 2.1: Summary of the WPT technologies in the literature

Technology	**Range**	**Nature**	**Frequency**	**Antenna devices**	**Applications**	**Papers**
Microwaves	Long	Radiative	GHz	Energy-radiating resonators, rectennas	Drone aircraft, satellite	[2], [18], [19]
CPT	Short	Nonradiative	kHz-MHz	Metal plate electrodes	Charging AUVs, low-power devices	[22], [23], [24]
IPT	Short	Nonradiative	kHz-MHz	Resonator coils	Charging AUVs, electric vehicles, smartphones, electric toothbrushes, laptop computers, and tablets	[17], [23] [25], [26], [29], [30], [31], [32], [33], [34], [35], [36], [37]

The review on IPT demonstrates that inductive wireless transmission systems have been studied more than CPT since there is a large amount of available literature containing comprehensive research on this technology. It has a broad spectrum of applications with various power levels [8] and can transmit power over longer distances than the CPT systems [39]. Considering the mentioned advantages of the inductive WPT systems, this thesis aims to adopt this technique for designing the wireless power transmission model for underwater applications.

Chapter 3 - Theoretical Framework

3.1 - Inductive Coupling Model

The IPT system generally consists of two sides: a primary (transmitting or transmitter, Tx) and a secondary (receiving, Rx). Figure 3.1 demonstrates the IPT system's circuit design. It can be observed that the coil L_1 at the transmitting side is directly connected to the power supply, whereas the coil L_2 at the receiving side is connected to the load.

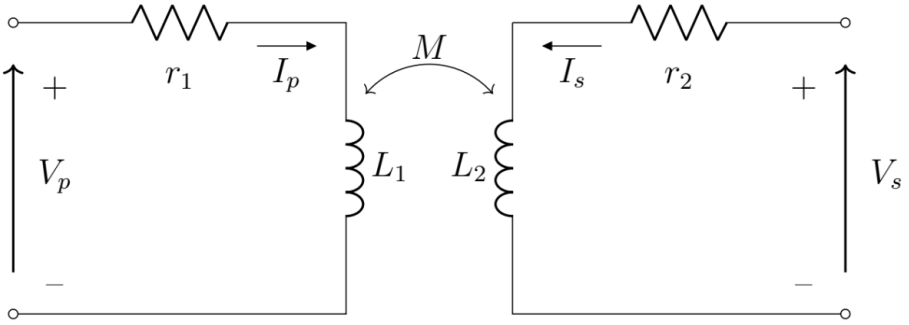

Figure 3.1: Inductive coupling model

At the primary side, a fluctuating electromagnetic field with frequency ω_p starts to be produced due to the current I_p. The frequency of this field is equivalent to the applied source voltage/current' one. The operational frequency of the IPT is typically within the kHz - GHz range, therefore the usage of frequency converters is required to ensure the input current/voltage matches the target frequency [40], [41]. In the circuit, M stands for the mutual inductance, as well as r_1 and r_2 denote the equivalent AC resistance of the coils. An equivalent circuit of the inductive coupling model is presented in Figure 3.2.

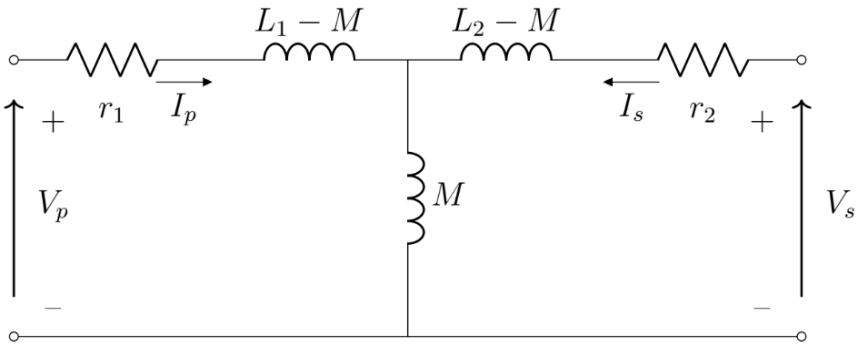

Figure 3.2: Equivalent circuit of the inductive coupling model (T-model)

By applying Kirchhoff's current and voltage laws, the following can be obtained:

$$V_p = [r_1 + jw(L_1 - M)]I_p + jwM(I_p + I_s)$$

$$= r_1 I_p + jwL_1 I_p - jwMI_p + jwMI_p + jwMI_s \quad (1)$$

$$= (r_1 + jwL_1)I_p + jwMI_s$$

$$V_s = (r_2 + jwL_2)I_s + jwMI_p \quad (2)$$

In matrix representation, the derived equations can be expressed as:

$$\begin{bmatrix} V_p \\ V_s \end{bmatrix} = \begin{bmatrix} r_1+jwL_1 & jwM \\ jwM & r_2+jwL_2 \end{bmatrix} \begin{bmatrix} I_p \\ I_s \end{bmatrix} \quad (3)$$

After denoting the corresponding matrices as **V**, **Z** and **I**, as well as canceling the imaginary parts of $Z_{11}(jwL_1)$ and $Z_{22}(jwL_2)$ the following expression can be obtained:

$$\mathbf{V} = \mathbf{Z} \cdot \mathbf{I} \quad (4)$$

3.2 - Mutual Inductance

If an electromagnetic field that is produced by one coil gets picked up by the second nearby coil, then a shared magnetic flux connects them together [42]. In such a case, there is a mutual

inductance between these two coils. The mutual inductance when there are no losses can be represented as

$$M = \sqrt{L_1 \times L_2}\,, \tag{5}$$

where L_1 and L_2 denote the inductances of the coils on primary and secondary sides, accordingly [43]. This formula is more related to the transformers due to the presence of perfect coupling and the absence of flux leakage. When dealing with WPT, however, the shared magnetic flux is significantly influenced by the transfer distance or by the alignment of the coils. The energy transfer from one coil to another via mutual inductance is referred as inductive coupling coefficient, k:

$$k = \frac{M}{\sqrt{L_1 \times L_2}}\text{, where } k \in [0,1]. \tag{6}$$

It is generally stated in the form of a decimal number, however the percentage value is also utilized. Thus, the mutual inductance is,

$$M = k\sqrt{L_1 \times L_2}\,. \tag{7}$$

3.3 - Compensation Network Technologies

To reimburse the electrical defects of the system, a compensation network is used, which is designed for improving the power transfer efficiency. The main working principle of this network is diminishing the reactive power supply by resonating with its corresponding coil. The system's constant voltage and current source behavior can be achieved by using several compensation networks. In this regard, the requirement for the control system runs off. The enhancement of the power transfer efficiency is accounted for having zero reactive impedance, meaning no corresponding losses.

The compensation network is classified into mono- and multi-resonant, depending on the number of reactive elements. The former compensation consists of one reactive element and operates at one resonant frequency. There are four different topologies of mono-resonant compensations: Series-Series (S-S), Series-Parallel (S-P), Parallel-Series (P-S), Parallel-Parallel (P-P) [44]. The name of the topology refers to the capacitor's placement relative to the inductor, namely S and P denoting series and parallel, respectively. The voltage or current source behavior of the system is determined by the secondary capacitor: a system functions as a current source in parallel connection. Otherwise, in series connection it has a voltage source functionality.

Among all the mono-resonant topologies, S-S compensation has more applications owing to its simplicity in integration. Apart from that, the primary capacitor of this network is not dependent on the coupling coefficient or load. It is also important to note that due to S-S topology, it is possible to modify secondary and primary compensation independently, as well as to have a large tolerance for misalignments [45].

Multi-resonant compensation consists of several reactive components. It is implemented in LCL and LCC topologies. The latter is generally utilized in sophisticated systems due to its power efficiency, maintaining constant values throughout a high misalignment in both horizontal and vertical axes [46]. This topology makes the system cost effective since it does not require a high cross-section area of conductors. However, S-S is more efficient than LCC topology since low number of elements in a circuit leads to lower voltage drop.

In this work, S-S compensation is used due to mentioned advantages. The circuit of the S-S network compensation is depicted in Figure 3.3. By using means of equations with mesh analysis, the expressions for source V_1voltage and load voltage V_2 can be derived:

$$V_1 = (R_1 + j\omega L_1 + \frac{1}{j\omega C_1})I_1 - j\omega M I_2 \tag{8}$$

$$V_2 = [(R_2 + j\omega L_2)I_2 - j\omega M I_1] = (R_L + \frac{1}{j\omega C_2})I_2 \tag{9}$$

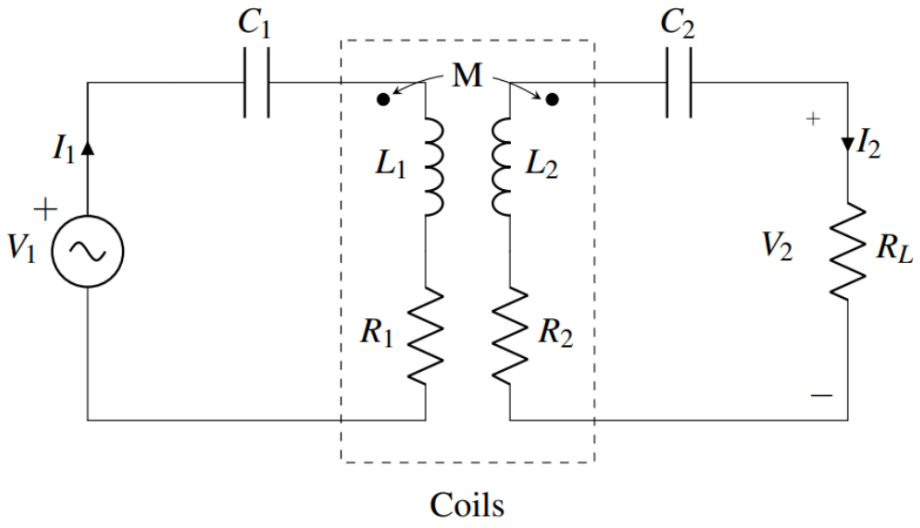

Figure 3.3: The circuit of S-S topology

From these equations, the following can be determined, where Z_{in} denotes the input impedance:

$$Z_{in} = \frac{V_1}{I_1} = R_1 + j(\omega L_1 - \frac{1}{\omega C_1}) + \frac{\omega^2 M^2}{(R_2 + R_L) + j(\omega L_2 - \frac{1}{\omega C_2})} \tag{10}$$

Terms, which are reactive, have to be canceled for having ohmic input impedance, meaning:

$$\omega L_1 - \frac{1}{\omega C_1} = -Imag[\frac{\omega^2 M^2}{(R_2 + R_L) + j(\omega L_2 - \frac{1}{\omega C_2})}] = \frac{\omega^2 M^2 (\omega L_2 - \frac{1}{\omega C_2})}{(R_2 + R_L)^2 + j(\omega L_2 - \frac{1}{\omega C_2})^2} \tag{11}$$

Therefore, we obtain the following:

$$\omega L_1 - \frac{1}{\omega C_1} = \frac{\omega^2 M^2 (\omega L_2 - \frac{1}{\omega C_2})}{(R_2 + R_L)^2 + j(\omega L_2 - \frac{1}{\omega C_2})^2} \tag{12}$$

This expression requires the primary side and the secondary of the circuit to resonate at one frequency. At resonance, $X_L = X_C$. Thus, the values of the resonant capacitor and inductors can be expressed as

$$\omega = \omega_0 = \frac{1}{\sqrt{LC}}, \tag{13}$$

where ω and ω_0 denote the operational and resonant angular frequency of the circuit, respectively. Since the resonant frequencies of primary and secondary sides have to be concordant with each other for high power transfer efficiency:

$$\omega_0 = \frac{1}{\sqrt{L_1 C_1}} = \frac{1}{\sqrt{L_2 C_2}}, \tag{14}$$

where L_1 and C_1 refer to the inductor and capacitor values on the primary side, whereas L_2 and C_2 represent the inductor and capacitor values on the secondary side, accordingly.

The inductance value of any manufactured coil can be measured at the specific frequency. Therefore, the value of the compensating capacitor can be determined via

$$C = \frac{1}{\omega_0^2 L}. \tag{15}$$

3.4 - Power Transfer Efficiency of Series-Series Topology

Power transfer efficiency is the ratio between input and output power. The power the load receives represents the former variable, whereas the power generated by the voltage source represents the latter:

$$\eta = \frac{R_L I_2^2}{R_1 I_1^2 + R_2 I_2^2 + R_L I_2^2} = \frac{R_L}{\frac{R_1 I_1^2}{I_2^2} + R_2 + R_L} \tag{16}$$

Using the load voltage V_2 expression, the ratio of current I_1 and I_2 can be identified:

$$\left|\frac{I_1}{I_2}\right| = \frac{R_2 + R_L}{\omega_0 M} \tag{17}$$

Therefore, the power transfer efficiency of the system is:

$$\eta = \frac{R_L}{R_1 \left(\frac{R_2 + R_L}{\omega_0 M}\right)^2 + R_2 + R_L} \tag{18}$$

3.5 - Eddy Current Losses

As was explained earlier, Faraday's Law of induction states that currents are induced inside the conductor due to an alternating magnetic field in this conductor. These currents travel in closed loops inside the conductor, normal to magnetic fields that create them. Such current loops are called eddy currents. These eddy currents are similar to the patterns observed on the water's surface while rowing.

The seawater and its increased conductivity results in eddy current losses in this environment. This, in its turn, leads to the reduction of the power transfer efficiency. Hence, all the aspects of the seawater medium have to be taken into account when designing the UWPT system. The increase in

operational resonant frequency causes more eddy current losses in seawater, therefore considerably high frequencies have to be avoided.

The impedance model was established in [47] which can be utilized to create an equivalent circuit for the underwater WPT system by employing Z-parameters. Hence by using the suggested equivalent circuit, eddy current losses can be properly anticipated. They can be defined as the difference of the total loss in seawater and in air:

$$P_{Eddy} = P_{loss,seawater} - P_{loss,air}\,. \tag{19}$$

Thus, the eddy current losses can be represented as a resistor. A study by [22] has a more detailed analysis of the detuning in water utilizing the Maxwell's equations and the eddy current losses.

3.6 - Water Properties

Water is known to be a naturally conductive environment. However, electric and magnetic fields encounter drawbacks in such conductive media since it causes an energy dissipation and, hence, reduction of the power transfer efficiency of the WPT systems. Therefore, it is important to consider the water properties when designing the UWPT. The conductivity value for the seawater usually ranges from $4\,S/m$ to $6\,S/m$ [48]. The latter parameter indicates that this seawater is more salty than the former one.

The material's ability to respond to the applied external electrical field is evaluated by electric permittivity. It describes the level of ease with which the electric field can flow through the material. Since water is polar, it is anticipated to have a high value of electric permittivity. According to [48], this value is generally determined by 81.

3.7 - The Circuit Model for the IPT in seawater

Since the IPT system is modeled for an underwater environment, an additional element is added to the system which represents the eddy currents induced in water. Hence, the seawater is introduced as an external object with an inductance and resistance. The resultant circuit of this system is represented in Figure 3.4. Here, L_{sw} and R_{sw} are the seawater's inductance and resistance. The transmitter and receiver parameters are denoted as L_t , R_t and L_r , R_r accordingly. There are three mutual inductances, namely M_{tr}, M_{rsw} and M_{tsw} that indicate the mutual inductances between the transmitter-receiver, seawater-receiver and transmitter-seawater, respectively.

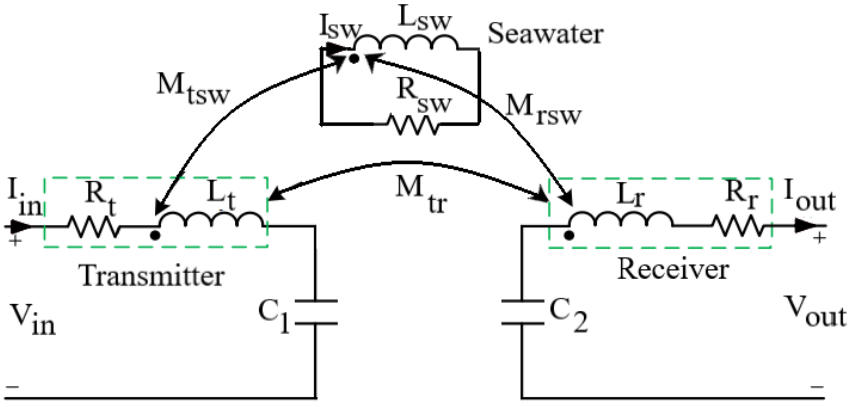

Figure 3.4: The circuit of S-S topology with an external object (seawater)

After applying Kirchhoff's voltage law, the following equations can be obtained:

$$V_{in} = Z_t I_{in} + j\omega(M_{tsw} I_{sw} + M_{tr} I_{out}) + Z_{C_1} I_{in} \tag{20}$$

$$-V_{out} = Z_{C_2} I_{out} + Z_r I_{out} + j\omega(M_{rsw} I_{sw} + M_{tr} I_{in}) \tag{21}$$

$$Z_{sw} I_{sw} + j\omega(M_{tsw} I_{in} + M_{rsw} I_{out}) = 0 \tag{22}$$

where the last equation is derived for seawater with the impedance Z_{sw}. Then, the following formulas are obtained, where each coil's self- and external object's reflected impedances are denoted by $Z_t^{'}$ and $Z_r^{'}$:

$$R_t^{'} = R_t + \frac{M_{tsw}^2 \omega^2}{|Z_{sw}|^2} \tag{23}$$

$$L_t^{'} = j\omega(L_t - L_{sw}\frac{M_{tsw}^2 \omega^2}{|Z_{sw}|^2}) \tag{24}$$

$$Z_t^{'} = R_t + \frac{M_{tsw}^2 \omega^2}{|Z_{sw}|^2} + j\omega(L_t - L_{sw}\frac{M_{tsw}^2 \omega^2}{|Z_{sw}|^2}) \tag{25}$$

$$R_r^{'} = R_r + \frac{M_{rsw}^2 \omega^2}{|Z_{sw}|^2} \tag{26}$$

$$L_r^{'} = j\omega(L_r - L_{sw}\frac{M_{rsw}^2 \omega^2}{|Z_{sw}|^2}) \tag{27}$$

$$Z_r^{'} = R_r + \frac{M_{rsw}^2 \omega^2}{|Z_{sw}|^2} + j\omega(L_r - L_{sw}\frac{M_{rsw}^2 \omega^2}{|Z_{sw}|^2}) \tag{28}$$

Then, the mutual inductance $Z_{tr}^{'}$, taking into account the seawater effect is:

$$R_{tr}^{'} = R_{sw} + \frac{M_{tsw} M_{rsw} \omega^2}{|Z_{sw}|^2} \tag{29}$$

$$M_{tr}^{'} = j\omega(M_{tr} - L_{sw}\frac{M_{tsw} M_{rsw} \omega^2}{|Z_{sw}|^2}) \tag{30}$$

$$Z_{tr}^{'} = R_{sw} + \frac{M_{tsw} M_{rsw} \omega^2}{|Z_{sw}|^2} + j\omega(M_{tr} - L_{sw}\frac{M_{tsw} M_{rsw} \omega^2}{|Z_{sw}|^2}) \tag{31}$$

Due to the effect of water, new terms are substituted into the imaginary and real parts of the impedances. As a result, the self-inductance is reduced, as well as the self-resistance is raised.

The power transfer efficiency of the underwater IPT system with seawater effect considered is:

$$\eta = \frac{P_{out}}{P_{in}} = \frac{R_L}{R_t' \left(\frac{R_L + R_r'}{\omega (M_{tr} - M_{sw})} \right)^2 + R_L + R_r'}, \tag{32}$$

where

$$M_{sw} = L_{sw} \frac{M_{tsw} M_{rsw} \omega^2}{|Z_{sw}|^2}. \tag{33}$$

Chapter 4 - Simulation Details

This chapter presents the methodology used for this research. The approach of this study is quantitative and simulation-based, meaning that a set of data was collected from the simulations and then analyzed. There are a number of platforms that can simulate in low frequencies, such as COMSOL Multiphysics, Computer Simulation Technology, and Ansys Maxwell. For this study, Ansys Maxwell software is used to model the required inductive power system. This software is employed to design two resonators, receiver and transmitter, to simulate them and obtain data. It is applied to simulate the harsh seawater environment and to evaluate the performance of the proposed WPT system in different scenarios, as well.

4.1 - Coil Design of the IPT System

The coils were designed in Ansys software. The software contains predefined primitive structures, which then can be altered to match the interest of the user. In other words, some geometry operations have to be conducted on a selected basic structure to achieve the final desired object. In such a way, the planar spiral coil was selected as the foundation structure. Next, this coil was modified to meet the design parameters presented in Table 4.1. These values were selected to achieve a resonance at 85 kHz, as well as a high efficiency at this resonant frequency.

Table 4.1: Coil parameters

Parameter	Symbol	Value	Unit
Number of turns	N	30	
Coil width	w	2	mm
Air gap	g	1.5	mm
Inner diameter of coil	d_{in}	162	mm

Outer diameter of coil	d_{out}	370	mm
Number of strands	n	100	
Diameter of Litz wire	d_{Lw}	0.1	mm
Transfer Distance	d	98	mm

The transmitter and receiver coils are modeled to be identical. Figure 4.1 demonstrates the dimensions and abbreviations of the coil, where d_{in} and d_{out} represents the inner and outer diameters of the coil, respectively. The coil width is denoted by w, and the air gap between adjacent turns is denoted by g. The distance between transmitter and receiver coils is d.

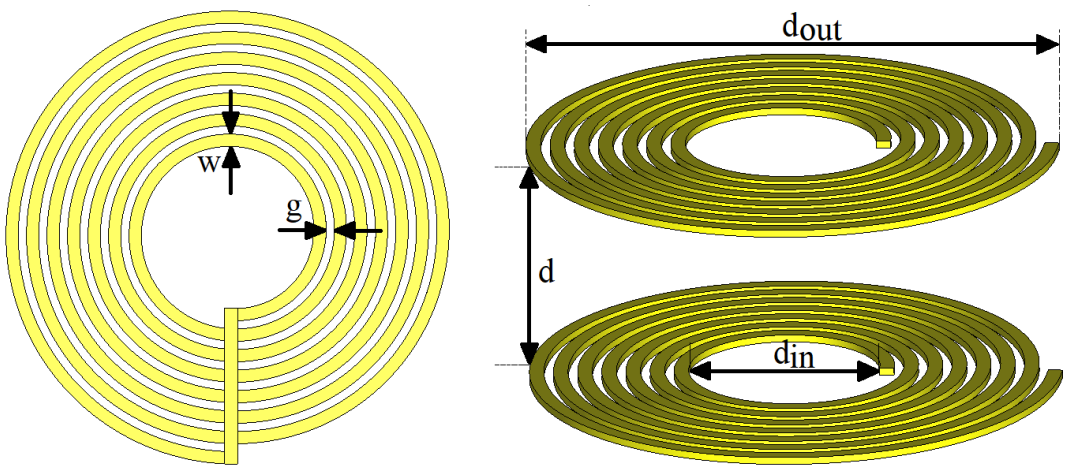

Figure 4.1: The coil design

Ansys software has several solution types categorizing into magnetostatic and electrostatic. Among all of them, particularly the eddy current solver was selected. Apart from that, Ansys Simplorer was applied for designing the complete circuit and obtaining the efficiency outcomes. Using Simplorer, the information on how the transfer efficiency changes with the frequency range can be obtained. Furthermore, since the software demands large system memory requirements, the mesh was changed for quicker run time. By enlarging the mesh size, the system achieves quick completion of the simulation, as well as requires less memory. However, this does not considerably

affect the results due to electromagnetic structures being less susceptible to mesh quality than mechanical or fluid mechanics models.

4.2 - Scenarios of the Simulation

The simulation study was conducted in three different scenarios, namely testing the proposed WPT system in various media, in a case with an external object between the transmitter and receiver, and in the presence of lateral misalignment. The former includes performing the simulation in air, seawater and more salty water environments. This can be done by adding a block region in the Ansys, and then adjusting its type of material. Table 4.2 demonstrates that the electrical characteristics of seawater, salty water and air as a transmission environment are not identical. Such cases demonstrate how the characteristics of the medium can influence and alter the electrical characteristics of the inductive WPT system, namely mutual inductances (M) and resistances (R_{mutual}), as well as the coupling coefficient (k). The system's performance in terms of power transfer efficiency is also analyzed in these mediums.

Table 4.2: Electrical parameters of different medium

Medium	Relative permittivity	Conductivity
Air	*1.0006*	$0\ S/m$
Seawater	*81*	$4\ S/m$
Salty water	*81*	$6\ S/m$

Misalignment of the receiver and transmitter resonators may occur as a result of the AUV movement due to instability under the water. Not perfectly aligned coils cause the reduction of the coupling coefficient. This, in its turn, results in decreased transfer efficiency. Therefore, the lateral misalignment study is also conducted in the seawater environment to evaluate the influence of

misalignment on the coupling coefficient of the WPT system. One of the two coils is shifted from the reference point while the second remains stationary. The displacement occurs in y-direction, ranging from $0 - 200\,mm$ with a step of $10\,mm$. Figure 4.2 demonstrates all the simulation scenarios.

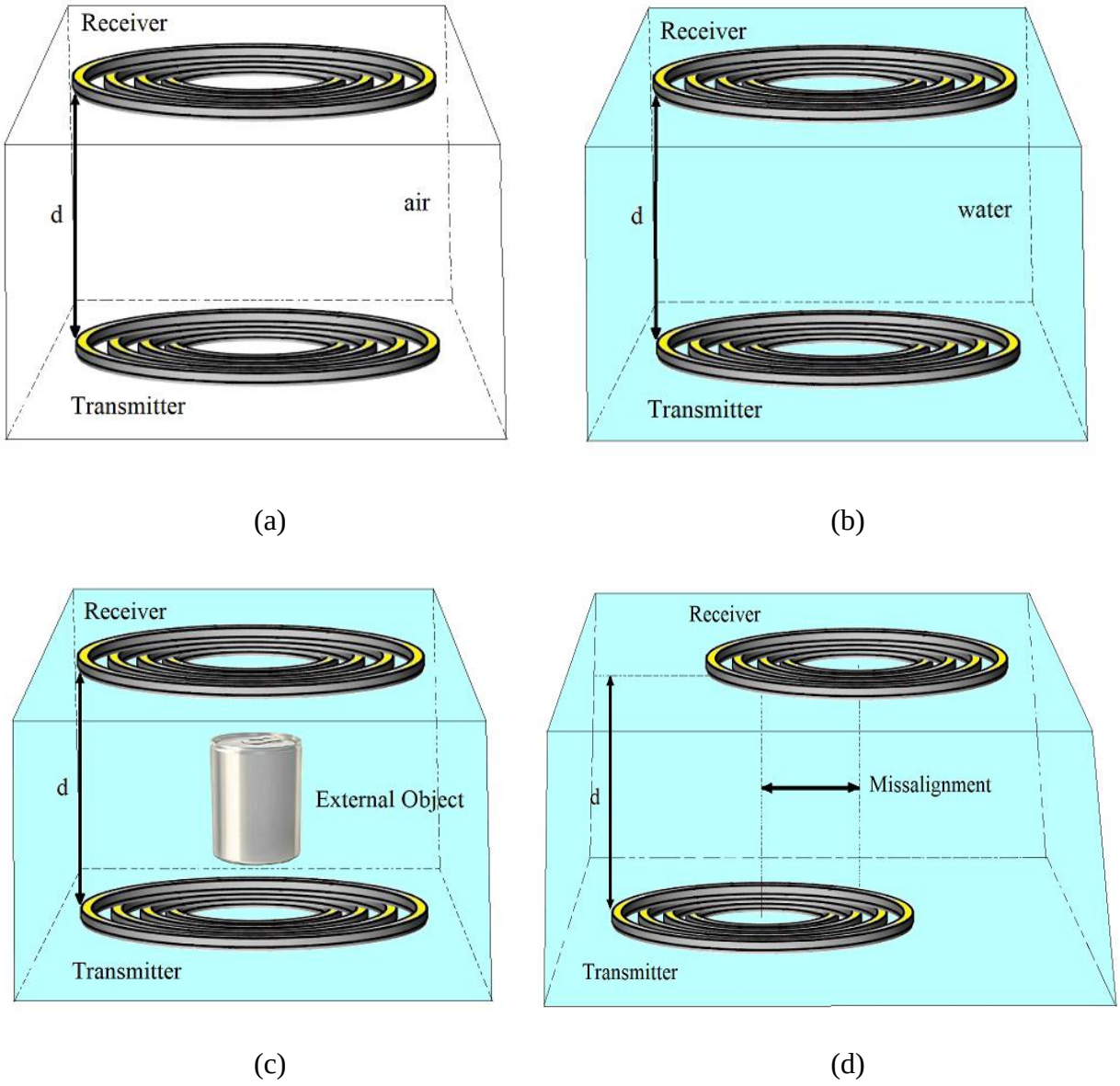

Figure 4.2: The simulation scenarios

In the case of an external object presence between resonators, different scenarios are taken into consideration. The external object in a real-case scenario can appear in the form of any foreign item

commonly used in the manufacture. The variety in samples includes different material, shape, dimensions, thickness, and positioning of the object, representing the real undersea environment, where these features are arbitrary. This process ensures that the simulation outcomes are consistent with the practical ones. Furthermore, the simulation of the aluminum block similar to a drink can is also conducted. The performance of the proposed system will be evaluated through the power transfer efficiency metric. Results of these scenarios are then compared with each other to have a general systematic representation.

4.3 - Object Selection

To assess the influence of nearby objects, materials whose effect on WPT systems wanted to be studied have to be chosen initially. There are several materials that have strong interaction with electromagnetic fields. Due to that interaction, the coil's electrical and magnetic properties are influenced. Therefore, the primary concern in the selecting procedure was to choose only that type of materials. The next part of the study was to concentrate on materials often utilized in the production of standard foreign items, such as coins or safety pins. These factors indicate that the main focus of this part of the study is metals. The knowledge acquired on the influence of various metals on UWPT coil characteristics would therefore serve as a reference point for investigating the effect of items that have these metals in their composition.

Due to their characteristics and atomic structure, metals have a considerable influence on the IPT system. This can be explained by their nature of being excellent conductors of heat and electricity because of the presence of moving free electrons in their lattices. Apart from that, the permeability of the metals are significant enough so the permeability of the coil's magnetic circuit

can be easily affected. For this reason, objects made of four different metals, i.e. copper, aluminum, nickel and iron, will be the subject of interest.

4.3.1 - Parameters of interest

For metal categorization, two metrics were taken into account: resistivity/conductivity, as well as relative permeability. The resistivity and conductivity are inversely proportional to each other, meaning that the metal's resistivity is the inverse of its conductivity. Based on the application, the choice of which one of these two variables can be utilized alternatively can be made. Thus, the metals having high resistivity have low conductivity, and vice versa: those with low resistivity have high conductivity. The metals used in this study with their properties can be found in Table 4.3. The Table consists of metals with various conductivity to investigate the effect of these different values of conductivity on the system's performance.

Table 4.3: Materials with their properties

Metal	**Type**	**Conductivity (S/m)$\times 10^7$**	**Relative Permeability**
Copper	Diamagnetic	5.8	0.999991
Aluminum	Paramagnetic	3.8	1.000021
Nickel	Ferromagnetic	1.45	600
Iron	Ferromagnetic	1.03	4000

The relative permeability is the ratio between a material's permeability and permeability of free space. The value of the relative permeability for the majority of nonmagnetic metals is approximately 1. However, as the metal becomes stronger and magnetic, i.e. ferromagnetic metals, its value can reach tens of thousands. Table 4.3 represents the relative permeability values of the selected metals. It is pertinent to note that the metals having relative permeability value of around

1 will be called non-ferromagnetic, while ferromagnetic metals are those, which have much higher permeability values.

4.3.2 - Metal Object Size

The objects that can influence the work of the WPT system generally can have different dimensions. Consequently, it is important to investigate the effect of metal plate dimension on coil characteristics. This can be done in relation to the geometry of the transmitter. The transmitter and receiver coils are identical in size in this study. The outer diameter of the coil is 370 mm and inner diameter is 162 mm. The initial concern for metal plate dimension was to have a large ("infinitely") plate. Such a plate can encompass the whole coil. In this situation, the optimal size of plate was determined to be $370 \times 370mm^2$, which is equal to the outer diameter of the coil. This includes the areas where the magnetic field is assumed to be more concentrated.

The second choice of the plate size was selected to be the half of the previous choice, meaning $185 \times 185mm^2$, which is larger than the inner coil diameter, meaning that the plate would interfere with the coil from the top view.

Then, it was of the interest to investigate the influence of much smaller sized metal plate, which is $90 \times 90mm^2$. Such dimensions indicate that the plate is located inside the coils (from top view), not interfering with them.

4.3.3 - Thickness of the Metal Objects

For the vast majority of the simulations, the thickness of the metal plates was set to 1 mm. Thereafter, for the instance of different metals, additional two thicknesses were tested: 3 mm and 5mm. Thus, three thicknesses were chosen for validating a hypothesis made during the study of the power loss formula of Bertotti: as long as the metal's thickness is larger than the skin depth, its thickness has no crucial effect on the power loss due to eddy currents produced in this metal [22].

4.3.4 - Shape of the Metal Objects

To determine the influence of shape of the metal plate on the performance of the inductive WPT system, two particular shapes were chosen, namely square and circular. Figures 4.3 and 4.4 depict the trimetric and side views of the IPT system while circular and square shaped external objects are placed between the transmitter and receiver.

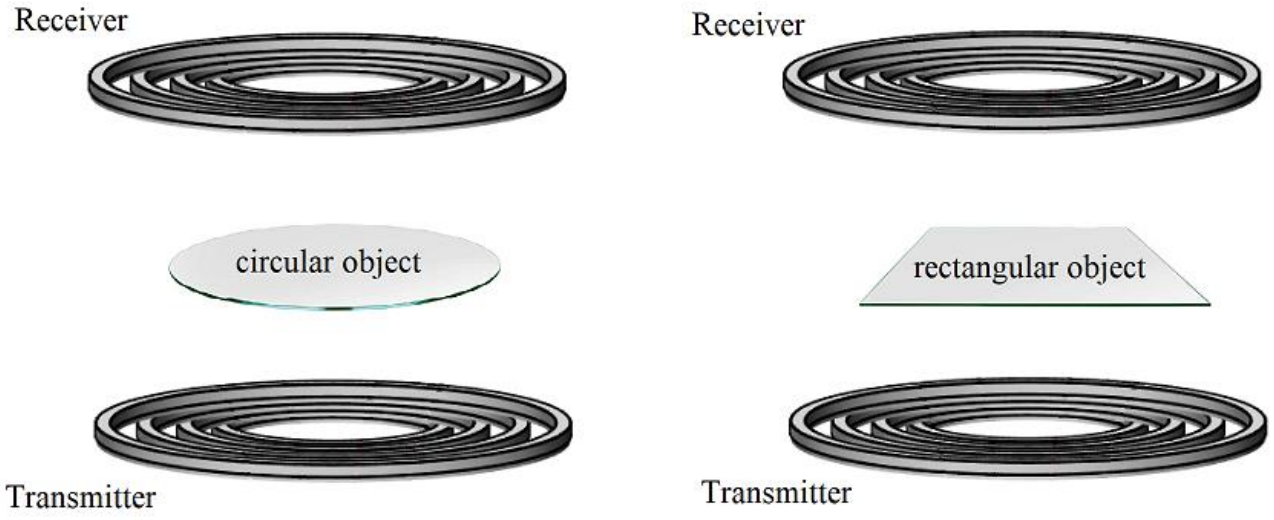

Figure 4.3: The external object between Rx and Tx: Trimetric view

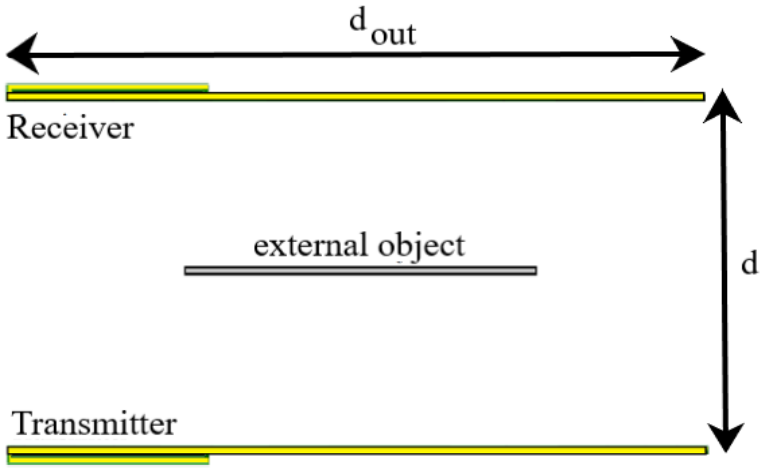

Figure 4.4: The external object between Rx and Tx: Side view

The dimensions of the square plate are $185 \times 185\ mm^2$, while the diameter of the circular plate is $185\ mm$. Such parameters are given to test the samples in "equal" condition, meaning that the size of two shapes corresponds to each other. The thickness of the plate for both shapes is $1\ mm$. The object is located right in the middle of transfer distance and at the origin from the top view.

4.3.5 - Position of the External Object

For these simulations, the external object had only one dimension of $185 \times 185mm^2$. The choice of selection was made based on the fact that the plate with mentioned size would interfere with the coils from top view but would not cover the entire coils. The metal plate had four positions with regard to coils: right at the center, shifted to the half of the coil's outer diameter value, shifted to the approximately fourth of the coil's outer diameter value and shifted completely out of the coil. These four positions can be observed in Figure 4.5 below.

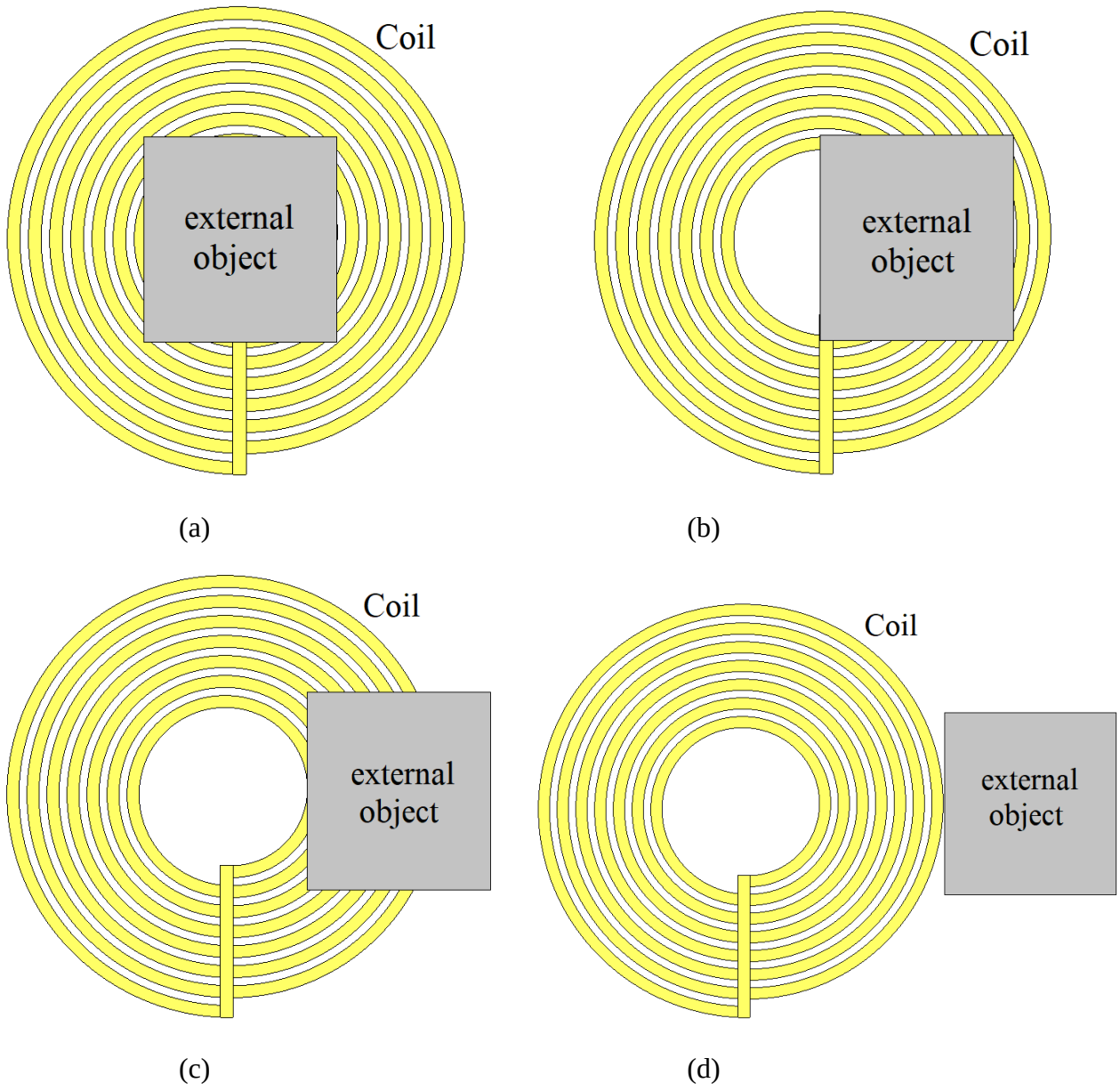

Figure 4.5: The positioning of the metal plate: top view

4.4 - Aluminum Can Simulation

The previous studies tested the metallic objects that are parallel to the coils. In order to investigate the effect of the vertical metal object, an ‘aluminum can’ is placed between the transmitter and receiver. It is made of aluminum and appears as a can to recreate a scenario where

a disposable container for food packaging appears as an obstacle to the system. The diameter of a standard can is *66 mm*, so is the diameter of this aluminum block. The height is *50 mm*.

To analyze the impact of the vertical metallic object on the performance of the inductive WPT system, the influence of the differently arranged aluminum obstacle is investigated. The three different arrangements can be observed in Figures 4.6, 4.7 and 4.8. For the first placement, the can is located right at the center of the system.

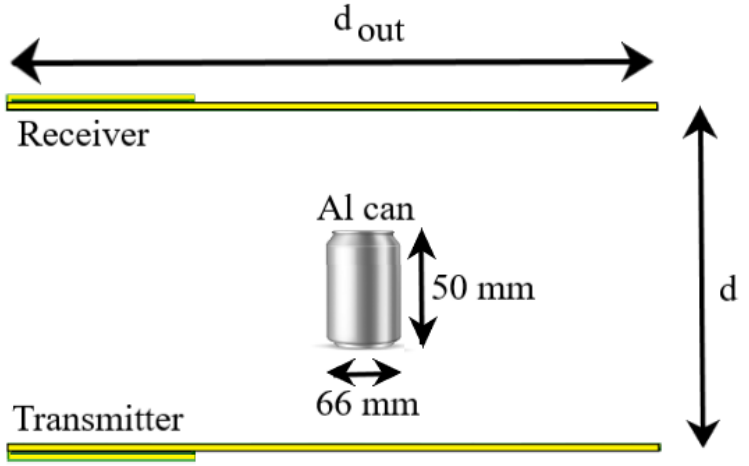

Figure 4.6: The first positioning of the aluminum can

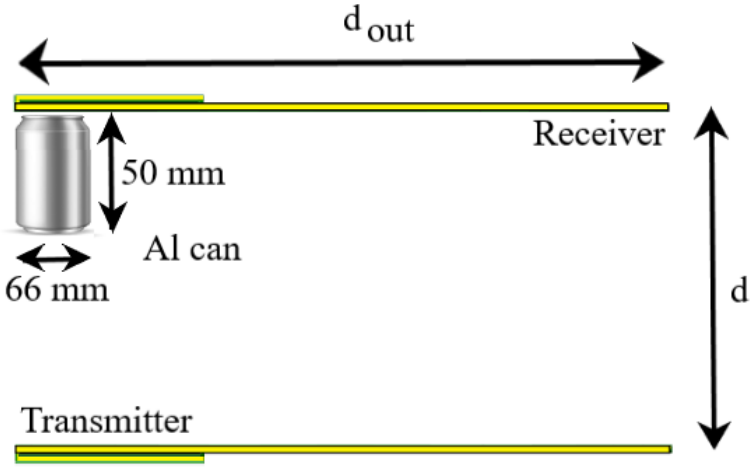

Figure 4.7: The second positioning of the aluminum can

Then, the can is placed to the left side, near to the receiver coil. Third location comprises an arrangement to the right side, near to the transmitter coil. All the three cases are simulated in seawater medium with a bulk conductivity of $4\ S/m$.

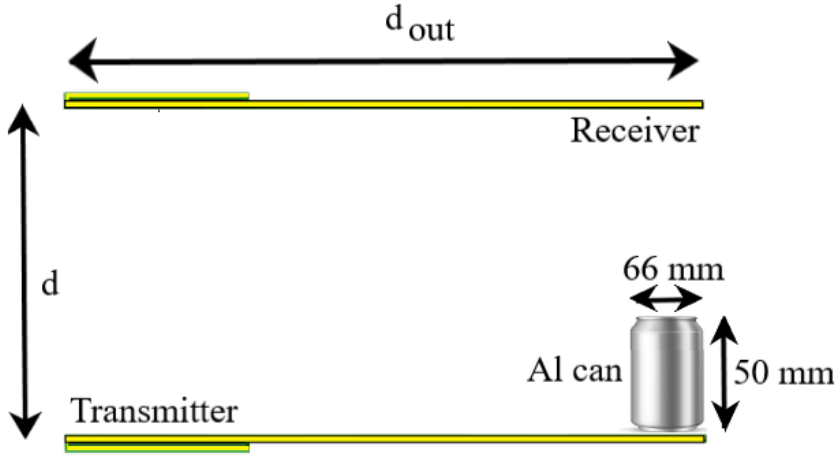

Figure 4.8: The third positioning of the aluminum can

Chapter 5 - Results and Discussion

5.1 - The WPT System Parameters

The results obtained from the simulations in Ansys Maxwell are presented in this chapter. The discussions are also given for the reported graphical outcomes, as well as the possible explanations for them. After simulating the proposed Ansys Maxwell, the results for the electrical parameters of the coil were obtained. These values for the sweater environment are presented in Table 5.1. Then, the parameters of the complete circuit components in Ansys Simplorer were fitted according to Table 5.2. This is required for calculation of the power transfer efficiency. To analyze how frequency affects the system performance, with each change in frequency, new values for compensation capacitors are determined.

Table 5.1: The electrical parameters of the coil for seawater ($4\ S/m$)

Parameter	Value	Unit
L_1	277.45	μH
L_2	277.57	μH
M	77.908	μH
R_{mutual}	552.96	$m\Omega$
k	0.28074	

Table 5.2: The parameters of the circuit components

Parameter	Value	Unit
f	85	kHz
C_1	12.65	nF
C_2	12.65	nF
R_{Load}	10	Ω

Amplitude of V_S	200	V
Magnitude of V_S	50	V
Phase of V_S	0	degrees

5.2 - Simulation of the IWPT in Air and Water Environments

Figures 4.1 and 4.2 demonstrate the efficiency of the IPT system over the change in frequency in air and water environments. The x-axis describes the frequency, while the y-axis represents the efficiency. It can be seen from Figure 4.1 (a) that the efficiency is deliberately increasing and reaches its maximum point at 50 kHz of 94.78%. After this point, the plot is slowly decreasing to 52.76% at 410 kHz. However, in Figures 5.1 (b) and 5.2 (a) the system performance experiences a sharp decrease without any raise in efficiency. For both cases, the maximum point is at 20 kHz of 95.44%. After this point, efficiency drops drastically, reaching 36.54% in seawater and 29.66% in salty water.

It is imperative to highlight that the seawater exhibits electrical conductivity, which in turn shows its potential to induce eddy currents at high frequencies. These eddy currents contribute to the rise of losses and impact the overall performance of the whole system. In this regard, the considerable decrease in the power transfer efficiency can be observed with the increase in frequency in seawater environments. Moreover, the relative permittivity of air is much lower than that of seawater. This results in an ease of electromagnetic waves propagation via air than via seawater. Hence, the electromagnetic fields produced by the transmitter do not face much resistance and attenuation when traveling through air, which explains the higher efficiency trend.

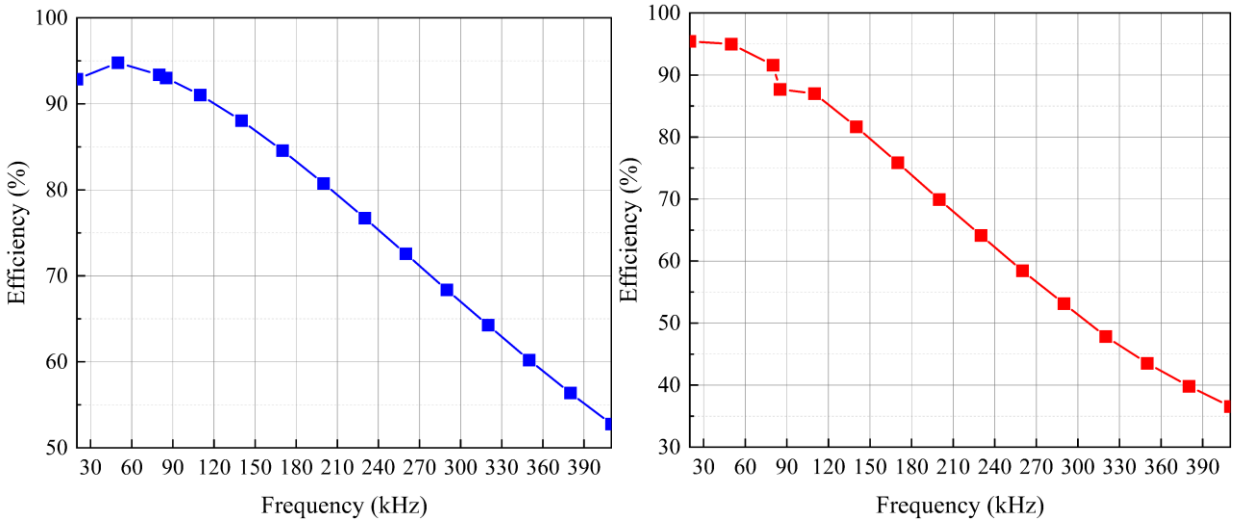

(a) Air medium **(b) Seawater medium**

Figure 5.1: The efficiency vs frequency graphs

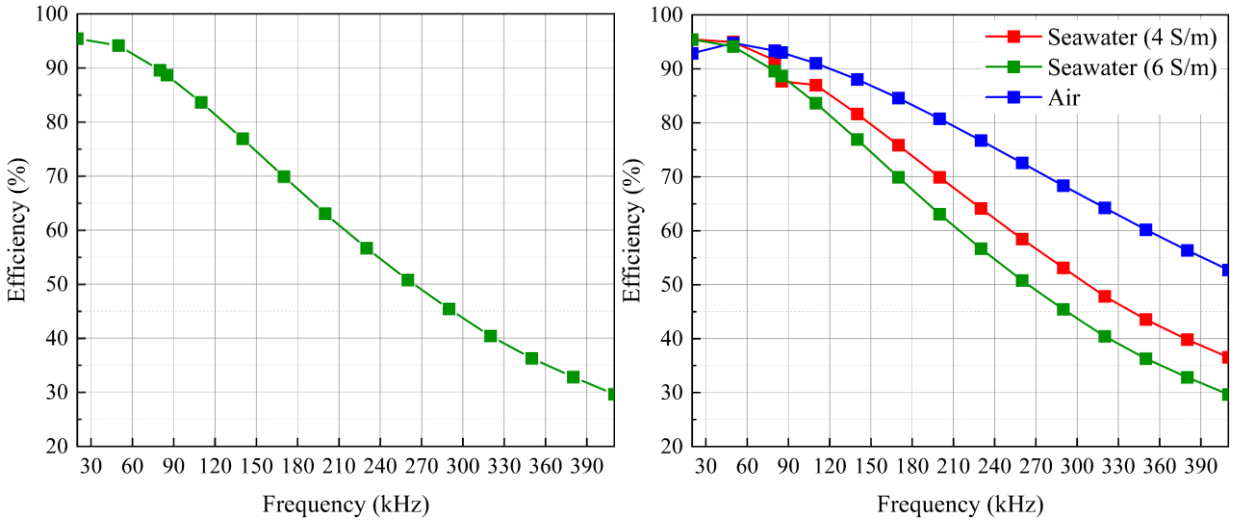

(a) Salty water medium **(b) All the mediums**

Figure 5.2: The efficiency vs frequency graphs

Figure 5.2 (b) demonstrates the change in the transfer efficiency in air, seawater and more salty water with frequency: blue representing the air, red - seawater, and green - more salty water. As can be seen from this graph, the decrease in efficiency in air is not as rapid as the other two. The most dramatic fall is related to the salty water, going down up to 29.66% at 410 kHz. Such a

difference can be explained by the fact that more salty water has a conductivity higher than the conductivity of seawater, meaning more eddy currents are generated with the increase of frequency. The observed pattern in efficiency change indicates that the frequency and system efficiency are nonlinearly related to each other. This validates the theoretical expectations of the power transfer efficiency equation for S-S compensation topology. The study in [32] claims that eddy current losses for the UWPT system experience a dramatic increase when the resonant frequency goes beyond a particular point, around 100 kHz. Based on this observation, it is reasonable to conclude that lower frequencies are more preferable for the inductive UWPT to achieve its high performance.

5.3 - Influence of Metal Plates on the UWPT

The coil inductance value in the seawater, when there is no any external object placed, is around 77.9 μH. This number is set as a reference value for the mutual inductance for further studies. It maintains reasonably constant throughout the whole frequency range, starting from 10 kHz to 200 kHz. Figures 5.3 demonstrates the mutual inductances of the coil when metal plates were placed between the transmitter and receiver of the UWPT system.

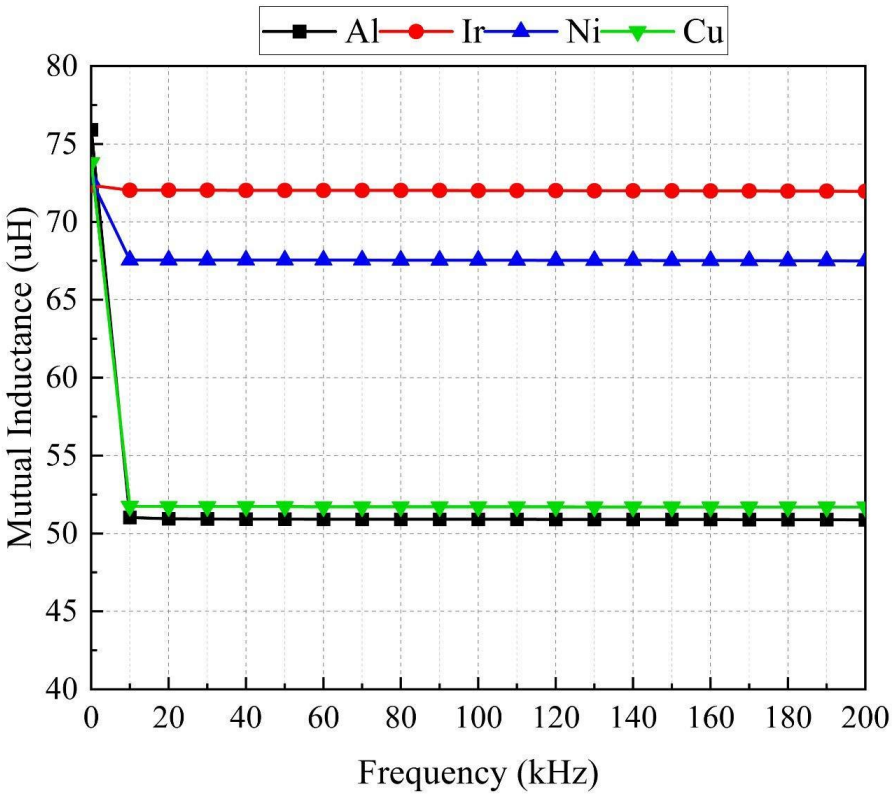

Figure 5.3: The mutual inductance over frequency for Cu, Al, Ir, and Ni

Placing copper and aluminum plates between transmitter and receiver coils caused the reduction of the mutual inductance value below the reference throughout the entire frequency range. The decline happens extremely fast until the frequency gets 10 kHz. Here, the simulation starts at a frequency of 0.06 kHz, as a default value in Ansys software. After that, the change in values happens considerably slowly, almost remaining stable up to 200 kHz. Initially, the ferromagnetic materials (iron and nickel) placement also decreased the inductance below the reference point and even below the inductance of the non-ferromagnetic curve. However, as the frequency increases, the drop occurs gradually, and at 10 kHz, it flattens out. The inductances for each case start to level off at one frequency. Prior to this value, the inductances of copper and aluminum cases are higher than of the remaining two; however after 10 kHz, the inductances of iron and nickel are closer to

the referencing value, whereas the inductances of copper and aluminum scenarios show a reduction of around 65% of the reference.

The possible explanation for such behavior is that at different frequencies, there are different dominating effects. To be precise, at low frequencies, the magnetization of the external metal plate happens due to the magnetic field of the coil. This, in turn, results in the rise of the magnetic flux through the resonator. Nickel and iron are ferromagnetic materials having high permeability values. High permeability feature leads to greater flux being induced onto the coil, meaning enhancing the mutual inductance of the coil. From Table 4.3, the relative permeability of iron is higher than the nickel's. When frequency starts increasing from 0 (DC), the eddy currents are induced in the external metal plate due to the coil’s alternating magnetic field. This causes a generation of another magnetic field opposing the other, hence lowering the inductance of the coil. Hence, at lower frequencies, the magnetization process prevails, meaning the enhancement of the inductance, while at high frequencies, the eddy currents dominate, which decreases the coil inductance.

Similarly, a high value of conductivity of the metal leads to a decrease in the inductance of the coil and vice versa. According to Table 4.3, copper is more conductive than aluminum. The possible explanation for this can be that due to high conductivity of metals, greater eddy currents are generated in them. This results in the generation of a stronger magnetic field opposing the exciting one. That is why the coil inductance lowers even further. Moreover, for the ferromagnetic material, the magnetization is hardly existent, being almost absent. Thereby, the placement of objects made of these metals drastically drops the inductance value of the coil.

Figure 5.3 demonstrates the mutual inductances of the coil when metal plates were placed between the transmitter and receiver of the UWPT system. For all the metals, placement of the metal plate raises the coil's mutual resistance above the reference value for all the metal types. In

particular, iron and nickel exhibit the largest increases among all. They achieve 2.67 Ω and 2.91 Ω at 200 kHz, respectively. As for the non-ferromagnetic metals, both demonstrate similar pattern, reaching to around 1.85 Ω at the same frequency.

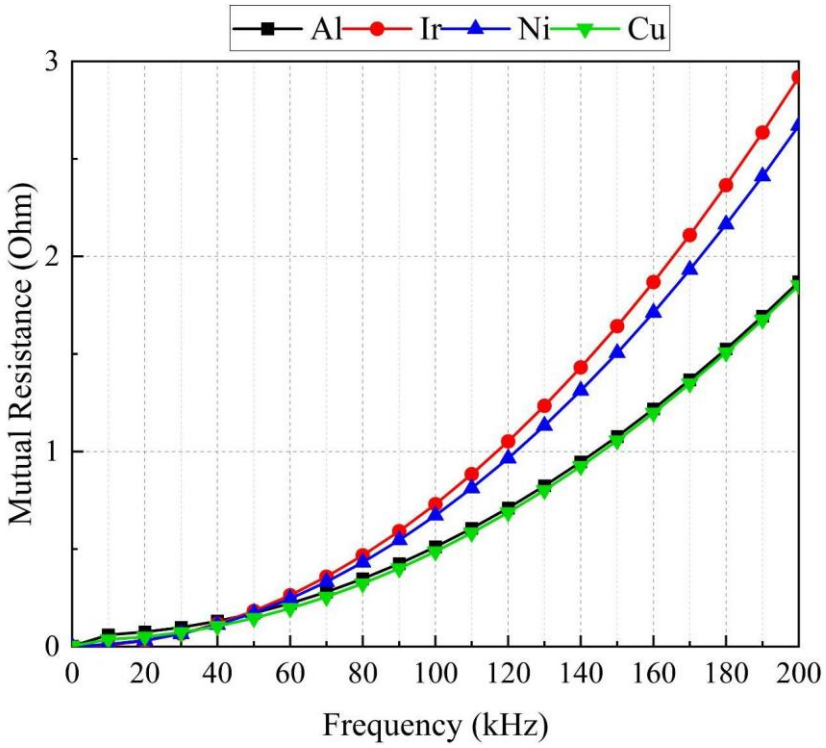

Figure 5.4: The mutual resistance over frequency for Cu, Al, Ir, and Ni

The formation of the eddy currents in the metal objects can interpret such a difference in the mutual resistance of the coil. It creates a magnetic field opposing the coil's driving current. As was explained in Chapter 3, eddy current losses can be represented as an additional resistor in the circuit. This results in the raise of the coil's effective resistance. One alternative explanation is that metal objects with higher conductivity have lesser resistance in structure, whereas those with lower conductivity already have more resistance. Hence, metals with low conductivity means more resistance, which, in its turn, means high mutual resistance of the coil. Therefore, non-ferromagnetic metals having higher conductivity, have low resistance, meaning the mutual

inductance of the coil increases slightly. For instance, copper and iron have different conductivity values which results in the trend in Figure 5.4.

It is pertinent to note that according to [9], there is a direct proportionality between the power transfer efficiency and the mutual inductance, which is also proportional to the coupling coefficient. Hence, low mutual inductance causes a deduction of efficiency of the system. Drop of inductance value observed in Figure 5.3 due to metal plate placement between two coils indicates that any obstacle reduces the power transfer efficiency, unless this object serves as a shielding mechanism for the system, an approach that utilizes reversed magnetic field in a conductor which is induced by eddy currents for decreasing the leakage magnetic field. Such a tendency of reduced performance of IWPT is expected in outcomes for the simulations in further scenarios.

5.4 - Influence of Metal Size on the UWPT

The simulation was performed to analyze the influence of the metal plate size on the performance of the UWPT. The key metric is power transfer efficiency through the defined frequency range. The sizes of the metal plate were $90 \times 90\, mm^2$, $185 \times 185\, mm^2$ and $371 \times 371\, mm^2$. All the materials were considered in this simulation. The results along with the outcome of bare coils (no external object) can be seen in Figures 5.5 - 5.8. Figure 5.5 represents the effect of the plate made of copper material on the power transfer efficiency of the proposed UWPT. Figure 5.6 demonstrates the effect of plates made of aluminum, Figures 5.7 and 5.8 show the influence of iron and nickel plates on the system performance, respectively.

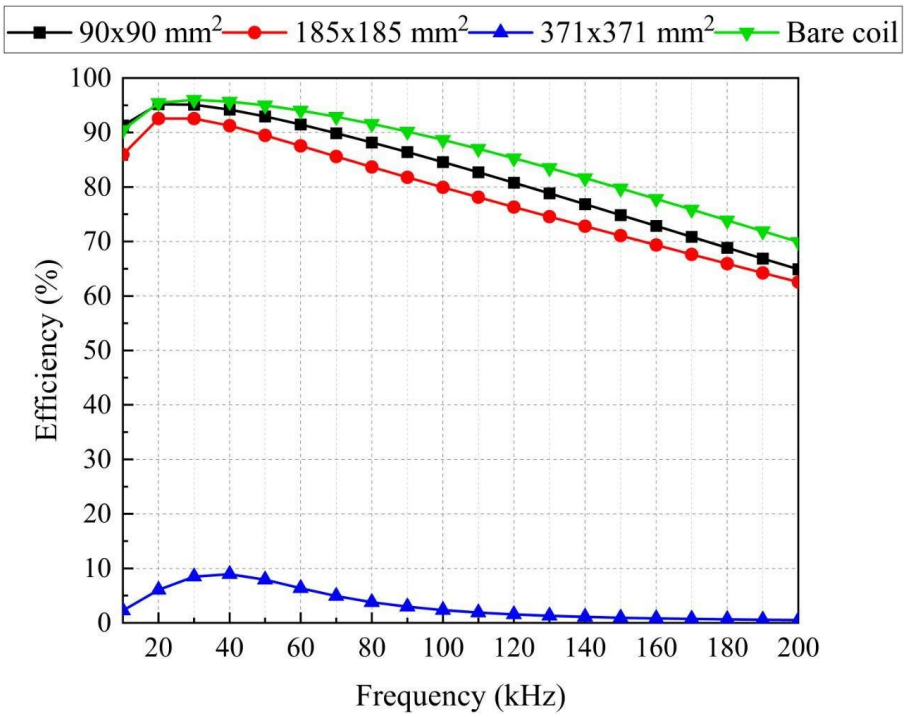

Figure 5.5: The effect of the copper plate size on the efficiency (at center location)

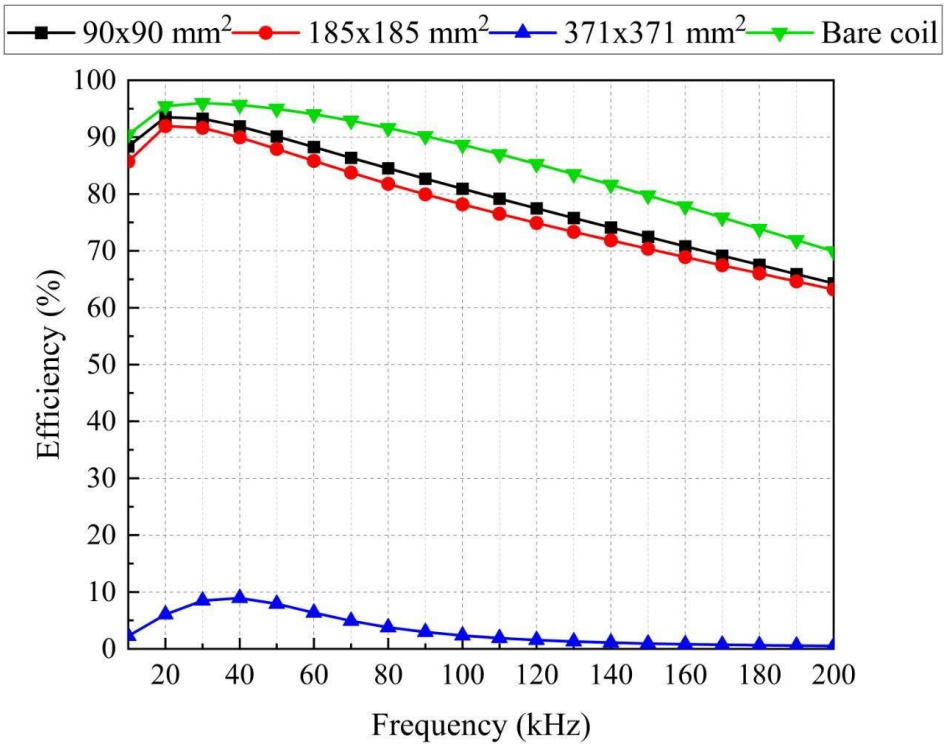

Figure 5.6: The effect of the aluminum plate size on the efficiency (at center location)

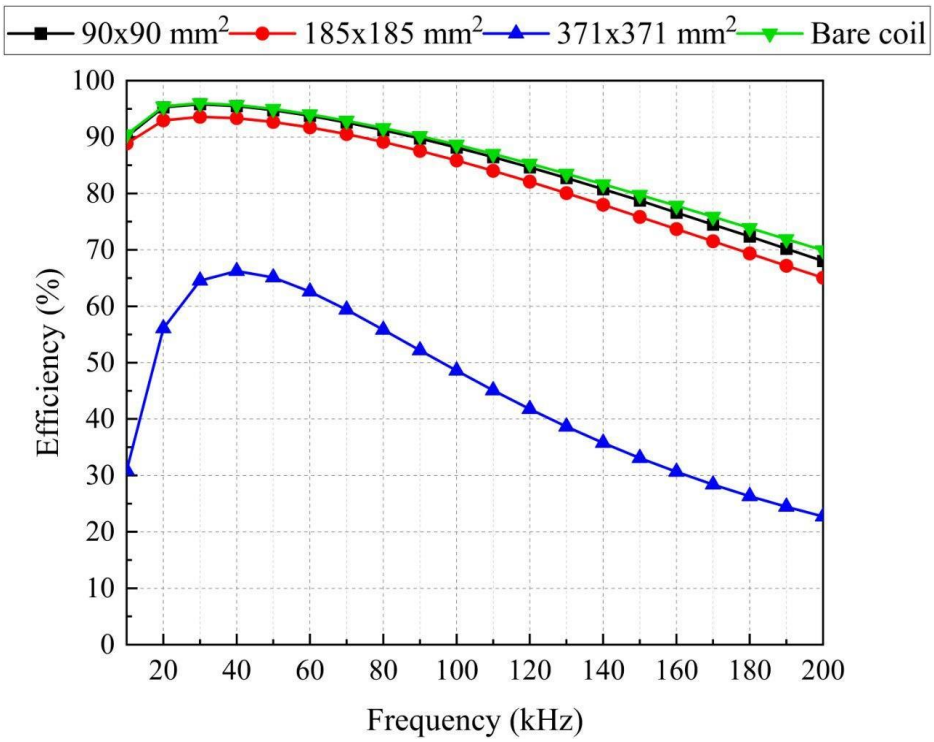

Figure 5.7: The effect of the iron plate size on the efficiency (at center location)

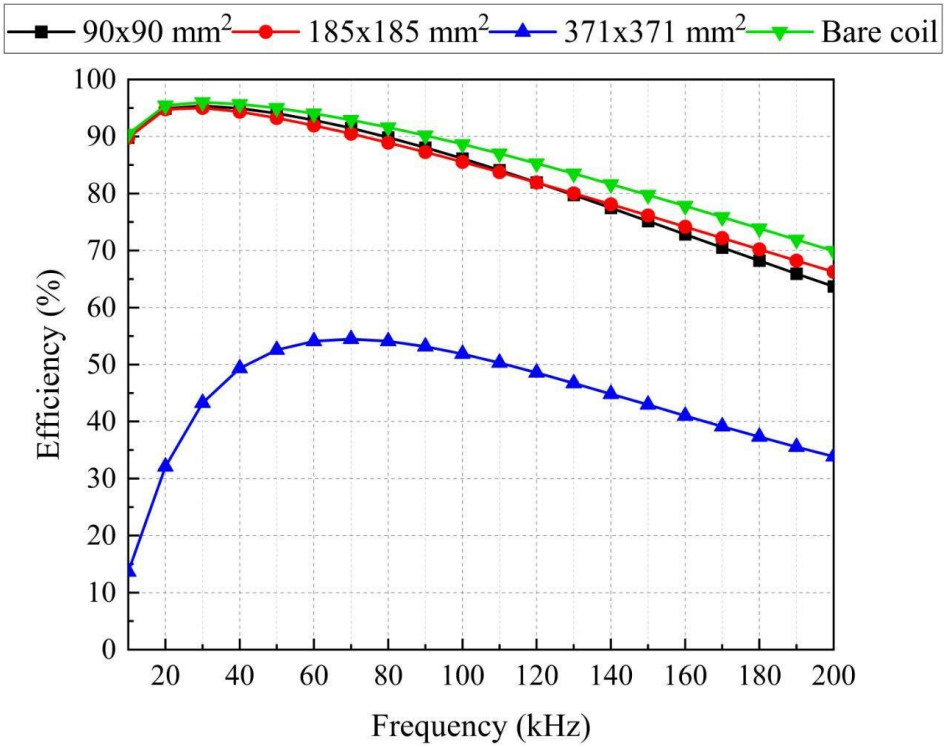

Figure 5.8: The effect of the nickel plate size on the efficiency (at center location)

As can be observed from the Figures, there are no considerable differences in the transfer efficiency between copper and aluminum plates, as well as between iron and nickel plates when the size of the metal plate does not fully cover the coil. $90 \times 90\ mm^2$ and $185 \times 185\ mm^2$ sized plates demonstrate similar influence on the system performance. However, as for $371 \times 371\ mm^2$ sized plates, a dramatic reduction in the efficiency was observed for all the cases. The aluminum and copper plates significantly decreased this metric, the maximum point appearing to be around 8.9% at 40 kHz, whereas the nickel and iron plates kept the efficiency at around 54% and 63% between 50 and 70 kHz. The iron plate with size $371 \times 371\ mm^2$ had the least effect on efficiency in comparison with other plates with the same size, which can be explained by its high relative permeability since it results in the decrease of the magnetic flux leakage around the receiving coil.

The possible explanation for this phenomenon is that a metal plate being in parallel position with the resonant coil leads to the main magnetic field of the transmitter being normal to the plate. This main magnetic field is loosened due to the magnetic field generated by the eddy current. Metal object with larger dimensions between the coils means increased magnetic flux passing via this object, leading to the more decreased main magnetic field. Such a process results in the degrading of the power transfer efficiency. This means that external metal plates with different sizes, that do not go beyond the coil size, do not substantially influence the performance of the inductive UWPT system for both ferromagnetic and non-ferromagnetic metals. Thereby, it can be concluded that the magnetic field above the resonator is tightly confined around it, meaning that the plate can have various sizes, as long as they are not greater than the size of the coil and do not fully cover it.

5.5 - Influence of Metal Position on the UWPT

For examining the effect of the metal plate position on the performance of the system, the plate size was set to $185 \times 185\ mm^2$ with a thickness of 1 mm. Such a choice of plate dimensions allows for flexible positions across the system. All the materials were tested to investigate the effect of each. Figures 5.9 and 5.10 depict the outcomes for the power transfer efficiency of underwater IPT systems under the influence of copper and aluminum plate positions, respectively. Figures 5.11 and 5.12 represent the outcome for the nickel and iron. It can be seen from the graphs that the location of the external object at the center of the coil accounts for the greater effect on the efficiency since the impact on the system performance decreases as an external object position further away from the coil's center.

These results can be interpreted by the distribution of the magnetic field between coils in the presence of metal objects, as depicted in Figure 1.1. It is apparent that in a considerable area in the middle of the system, the magnetic flux density is uniformly distributed. However, due to the metal object located in this area, the flux intensity behind this object is lower compared to that before it. This phenomenon happens by virtue of an induction of the reverse magnetic field due to eddy currents in a conductive object. Therefore, such a decline in the main magnetic field results in a reduction of the efficiency. As the plate moves from the central position towards the out, the area mainly susceptible to the uniformly distributed magnetic flux intensity becomes more open. Moreover, the flux direction in the outer edges of coil flows is nearly parallel with the metal plate. When the object is entirely out of the coil edge, only the leakage magnetic field is affected by the eddy currents in the metal. With all the listed factors, it is reasonable to conclude that the central position of a metal object affects the power transfer efficiency the most, hence a considerable reduction in efficiency can be observed in this case. Similarly, the system's least influenced

performance refers to the scenario when the object is located outside the coil, where the least differences in efficiency with the bare coil can be noted.

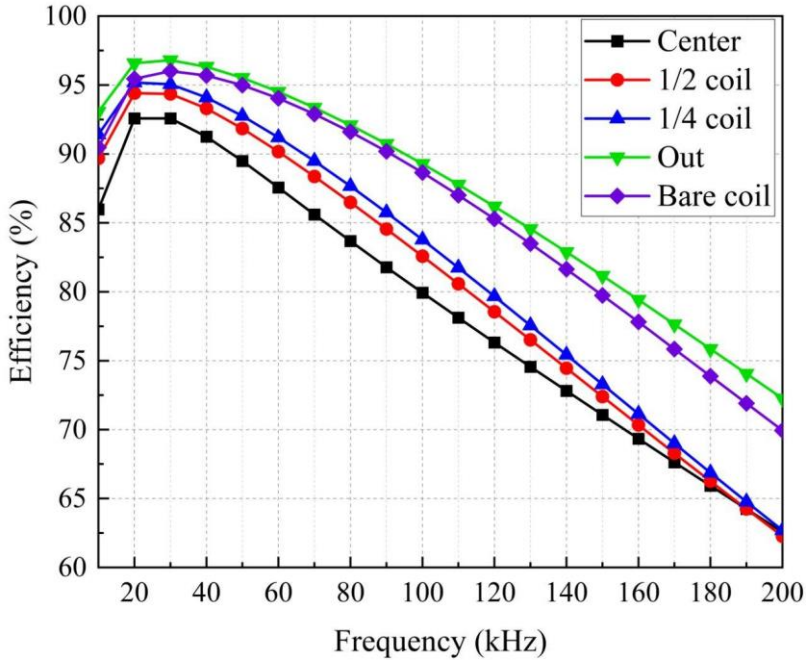

Figure 5.9: The effect of the copper plate position on the efficiency

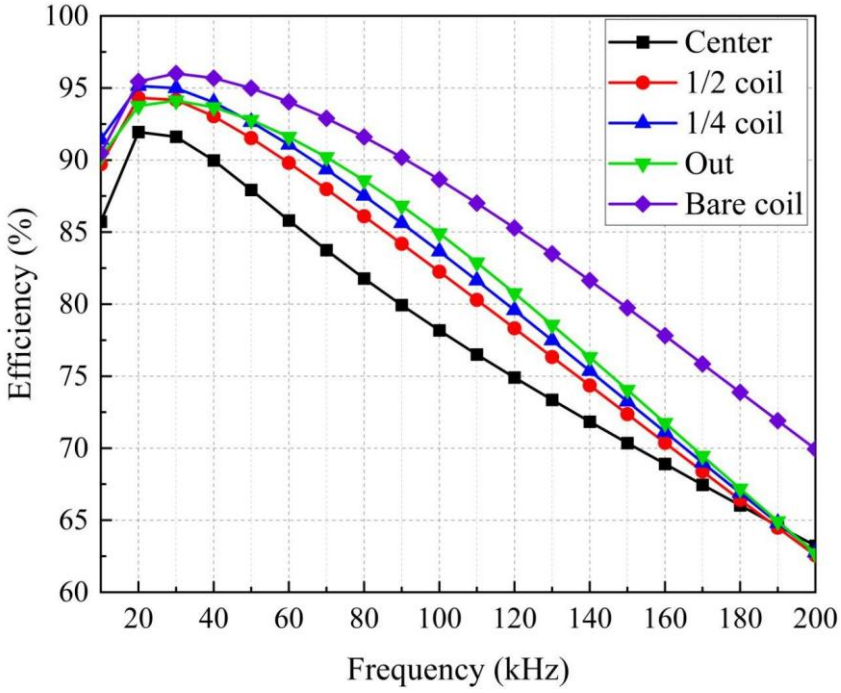

Figure 5.10: The effect of the aluminum plate position on the efficiency

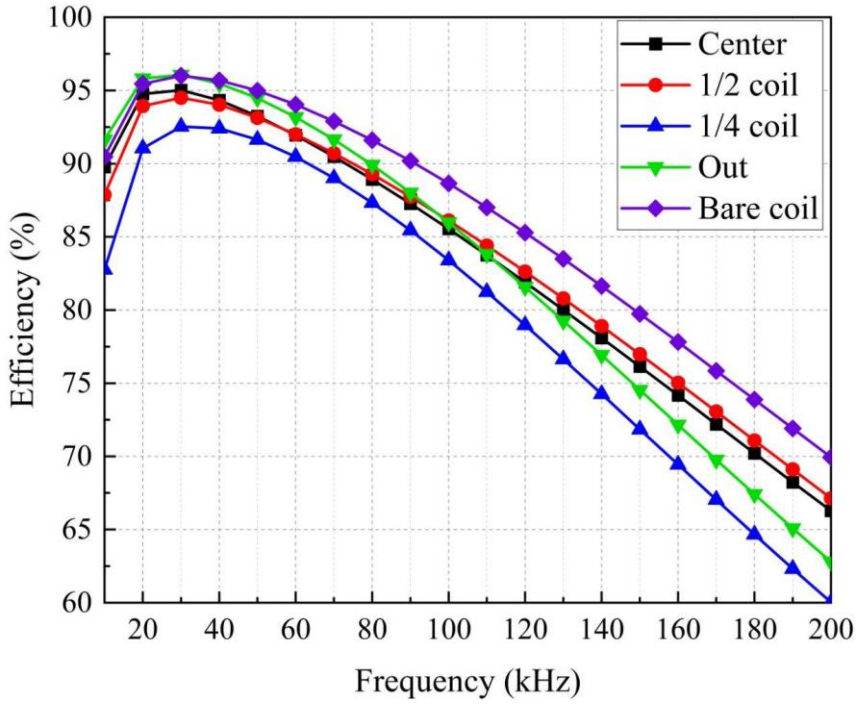

Figure 5.11: The effect of the nickel plate position on the efficiency

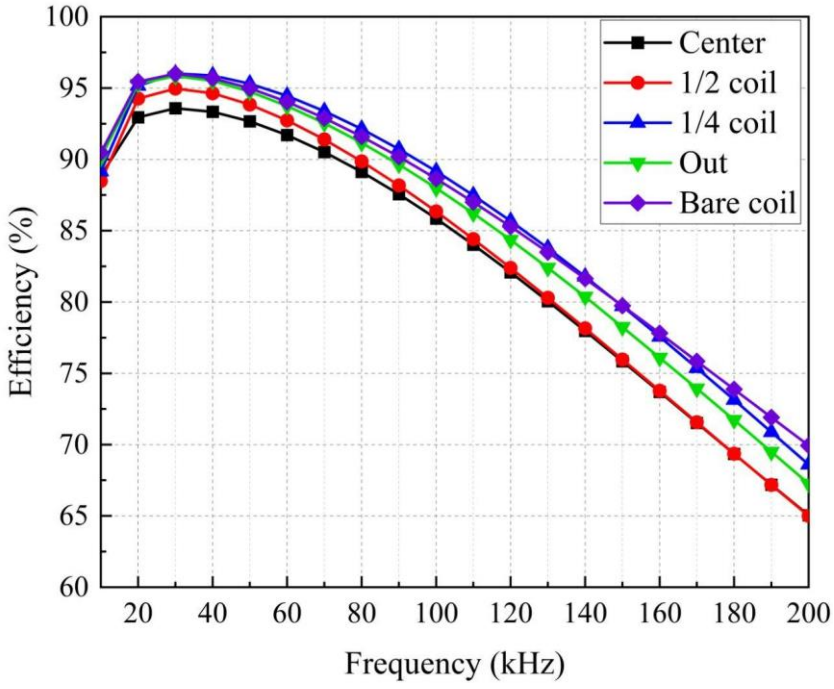

Figure 5.12: The effect of the iron plate position on the efficiency

The possible explanation for this behavior is that the $185 \times 185\ mm^2$ metal plate orients at the center of the coil and, hence, covers the coil area where the magnetic field has the highest concentration. In this case, the eddy currents start to be generated in the metal plate, significantly lowering the mutual inductance of the coil. When an external object is positioned away from the center (strong region), a less strong field acting on the plate causes lower eddy currents to flow. This results in a smaller effect on the system efficiency.

It is important to note that the specific positions of copper and iron plates resulted in an improvement of efficiency. From Figure 4.9, the WPT system experienced a rise in performance when the copper object was located out of the coil edge in comparison to the bare coil case. Similarly, when iron object was located in quarter of coil diameter, the blue line ($1/4D_{out}$) slightly exceeds the purple line (bare coil) and even intercepts it.

5.6 - Influence of Metal Plate Thickness on the UWPT

According to the power loss formula of Bertotti [22], the loss in power does not depend on the skin depth as long as the thickness of the metal is larger than the skin depth. To validate this claim, a metal plate with different thickness between the transmitter and receiver coils was simulated. Figures 5.13 and 5.14 represent the results obtained from the simulation of non-ferromagnetic materials, whereas Figures 5.15 and 5.16 depict the outcomes for the ferromagnetics. It can be observed from Figure 5.13 that various thicknesses of the copper object do not account for the greater effect on the efficiency. The curves demonstrate a similar pattern throughout the frequency range. However, for the aluminum, nickel and iron objects, the thickness of 1 mm resulted in a large influence on the system performance. When thickness was set to 5 mm, the increase in the efficiency occurred, as shown in the Figures 5.14, 5.15 and 5.16. From such observations, the following can

be concluded: as the thickness of the metal plates increases, the UWPT system performance enhances, meaning that the metal objects placed perpendicular to the coils (i.e. increase of the dimension in z-direction) contribute to the high performance of the wireless transmission system.

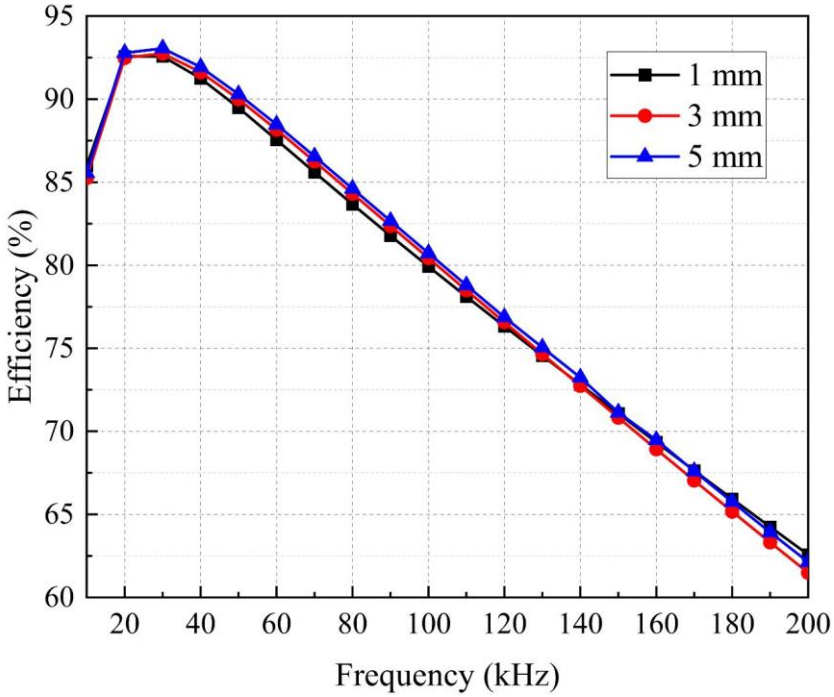

Figure 5.13: The effect of the copper plate thickness on the efficiency

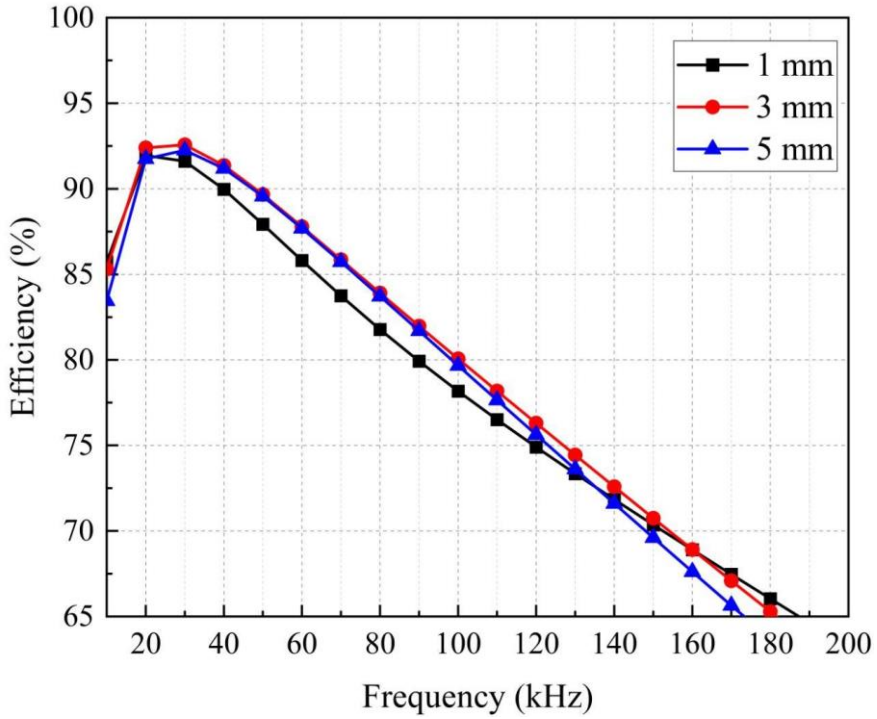

Figure 5.14: The effect of the aluminum plate thickness on the efficiency

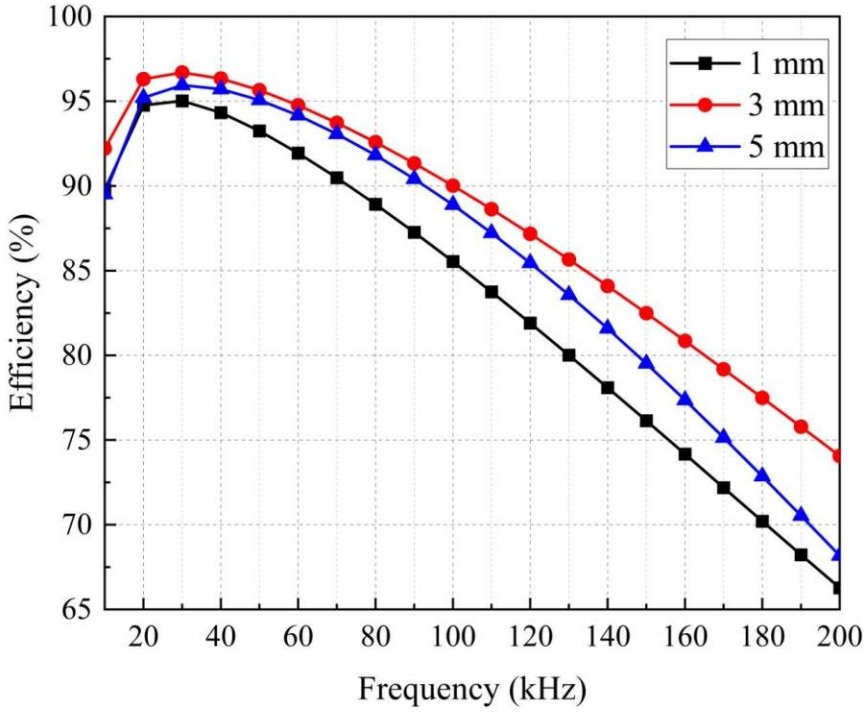

Figure 5.15: The effect of the nickel plate thickness on the efficiency

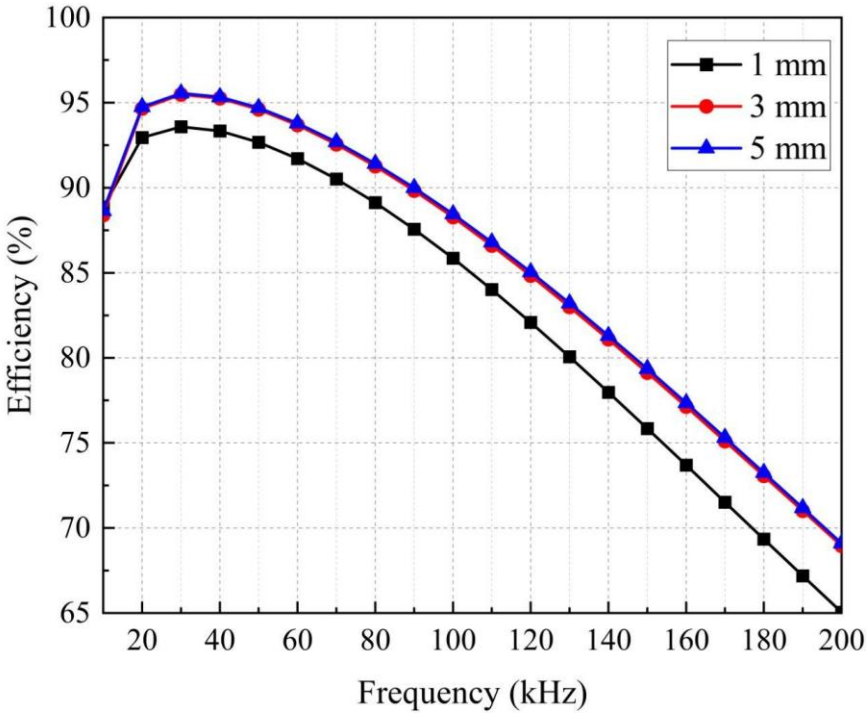

Figure 5.16: The effect of the iron plate thickness on the efficiency

The derived output can be interpreted by the magnetic field distributions. When the metal object is placed between the receiver and transmitter coils in perpendicular, it is located in parallel with the main magnetic field. In this case, eddy currents in the object are induced only due to the leakage flux passing through it. When eddy currents in the aluminum object generate a magnetic field, it disturbs the leakage flux so the magnetic field is not weakened. It, vice versa, improves the transmission of the main magnetic field a little. Therefore, the system performance is enhanced when the vertical object is present.

5.7 - Influence of Metal Plate Geometry on the UWPT

In this study, the influence of the external object geometry on the power transfer efficiency was analyzed. For this purpose, two shapes of the metal plate, namely circular and square were simulated. The results are presented in Figures 5.17, 5.18 and 5.19.

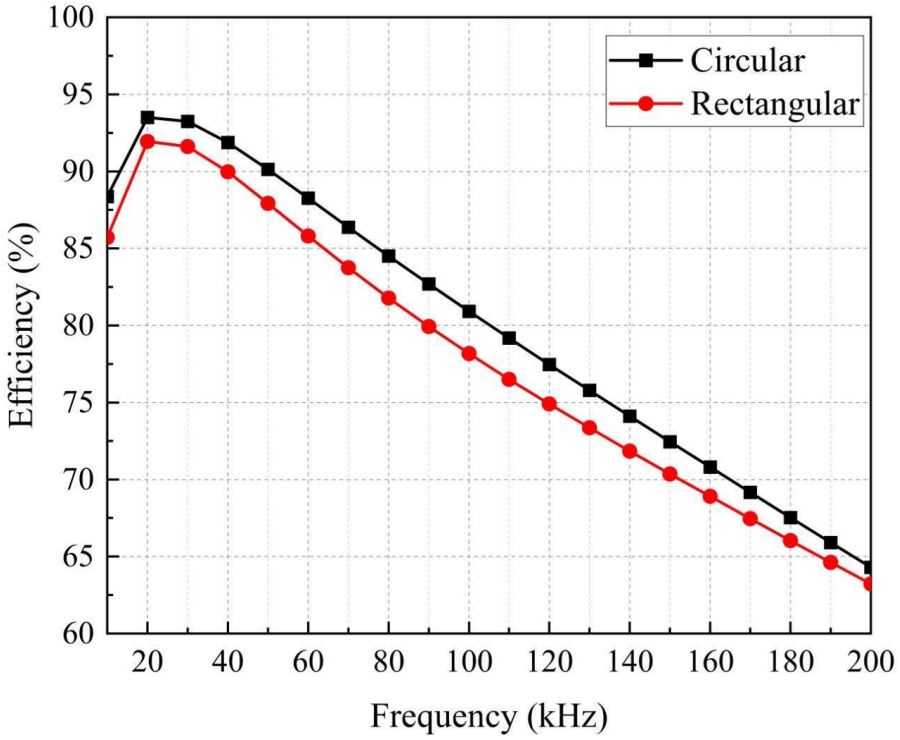

Figure 5.17: The effect of the aluminum plate geometry on the efficiency

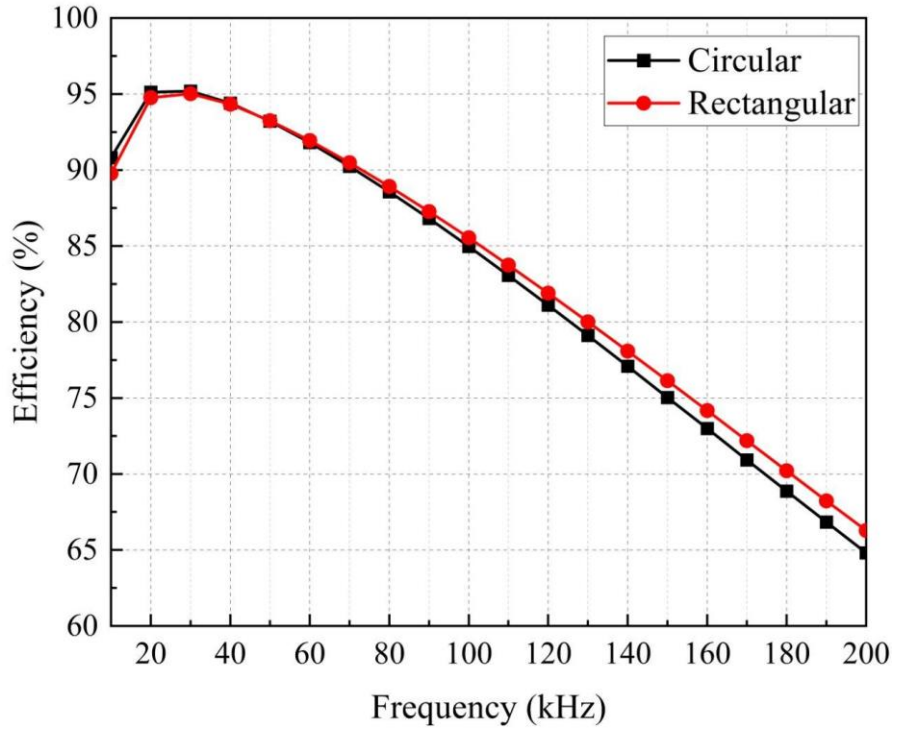

Figure 5.18: The effect of the nickel plate geometry on the efficiency

It is evident from Figure 5.17 and 5.19 that rectangular shaped plates have more effect on the performance of the system. The difference in efficiency for the aluminum plate is about 3%, while the difference for the iron plate is approximately 5%. Despite that, for the nickel plate, the curves in Figure 5.18 show a similar pattern up to 90 kHz. After that, they start to deviate from each other, having a difference of around 1.2%.

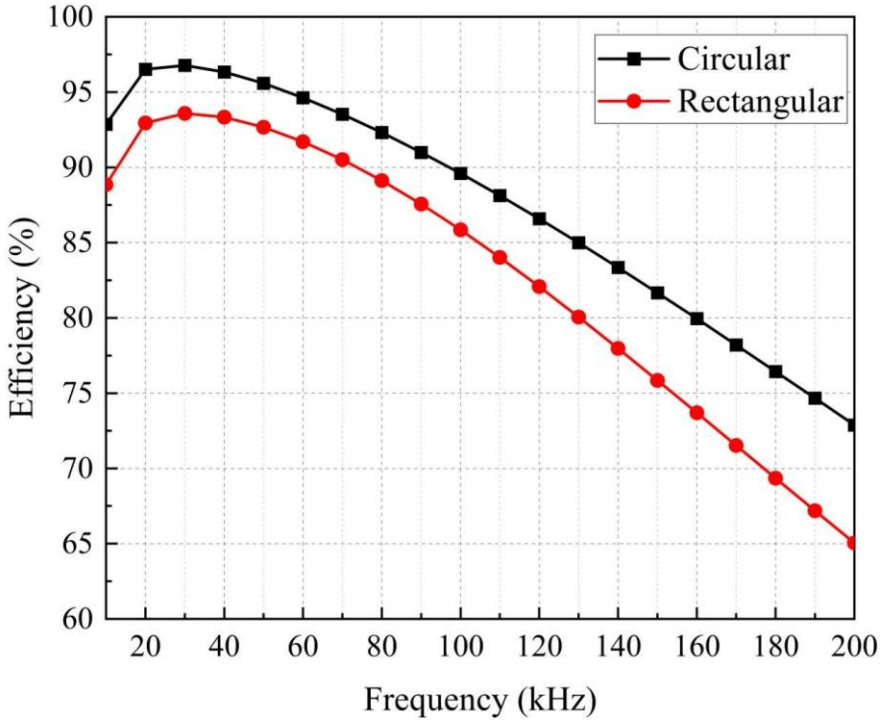

Figure 5.19: The effect of the iron plate geometry on the efficiency

5.8 - Influence of Aluminum Can on the UWPT

In this study, the influence of the aluminum can on the power transfer efficiency was analyzed. For this purpose, the can demonstrating the drink bottle, was placed between the receiver and transmitter. The results are depicted in Figure 5.20. It represents the outcomes for three different arrangements of the aluminum object. For the first placement, the can was located right at the center

of the system. Then, the can was placed to the left side, near to the receiver coil. Third location comprises an arrangement to the right side, near to the transmitter coil.

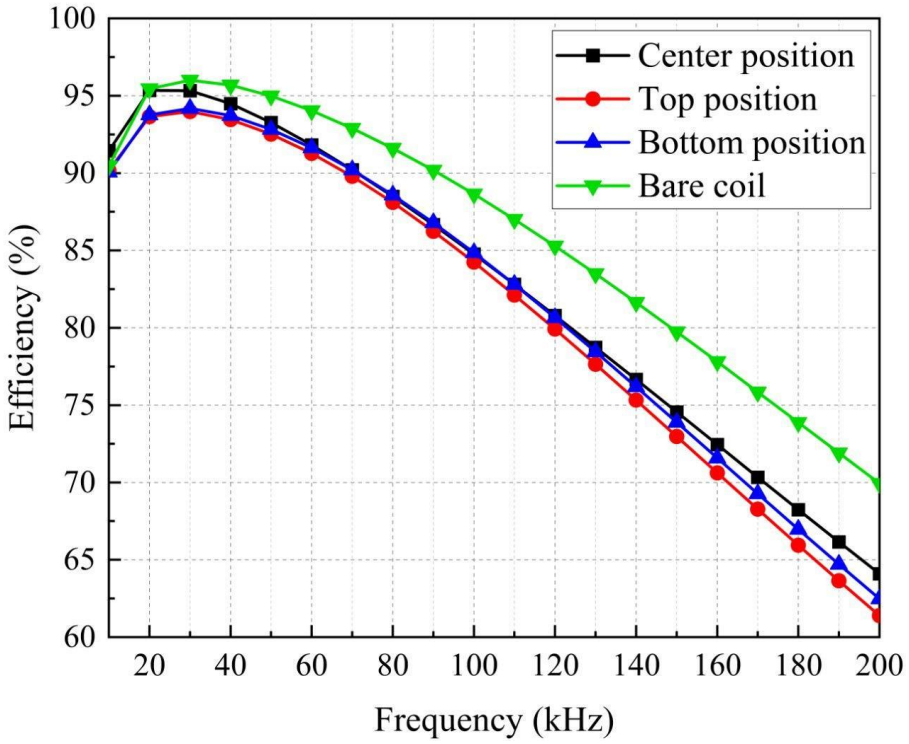

Figure 4.20: The effect of the Al can positioning on the efficiency of IPT

The graph contains a trendline for the bare coil also to compare the three cases with it. It can be observed that the placement of aluminum can decrease the efficiency of the system by about 5%. It is imperative to note that before the frequency reaches 40 kHz, the efficiency outcomes obtained for can placed right in the middle of coils represent similar values to those when there is bare coil, meaning no can. After this point, the trend approaches the same pattern of the remaining two cases. Red, blue and green lines do not considerably diverge from each other, meaning that the location of the aluminum can (middle, upper left, bottom right) do not significantly affect the performance of the system.

The possible explanation for this output is that both receiver and transmitter coils were designed symmetrical to simplify the modeling process. The presence of a slight difference in trend lines

indicates the effect of additional copper elements used to connect the ends of the coils. The location of the can to the side where these elements are present decreases the efficiency of WPT more than placement to the side where those are absent.

Table 5.3: Summary of findings

Case study	Finding
I	The electromagnetic fields produced by the transmitter do not face much resistance and attenuation when traveling through air. However, the eddy currents contribute to the rise of losses with the increase in frequency in seawater environments. More salty water has a conductivity higher than the conductivity of seawater, meaning more eddy currents are generated with the increase in frequency. The frequency and system efficiency are nonlinearly related to each other.
II	Increasing the distance of the receiver coil from the aligned position leads to the reduction of the coupling coefficient. This, in turn, results in a reduction in efficiency.
III	At lower frequencies, the magnetization process prevails, meaning the enhancement of the inductance, while at high frequencies, the eddy currents dominate, which decreases the coil inductance. Metal objects with higher conductivity have lesser resistance in structure, whereas those with lower conductivity already have more resistance. Hence, metals with low conductivity mean more resistance, which, in its turn, means high mutual resistance of the coil. The magnetic field above the resonator is tightly confined around it so that the metal object can have various sizes and affect the system's efficiency less, as long as it is not greater than the size of the coil and does not fully cover it. The central position of a metal object affects the power transfer efficiency the most and when it is positioned away from the center, it has a smaller effect on the system efficiency. The WPT system's performance can be enhanced when the vertical object is present. The rectangular-shaped plates have more effect on the performance of the system rather than the circular ones.
IV	The presence of an 'aluminum can' causes a degradation in the efficiency of the WPT system. However, a change in its position barely causes differences in outcomes since both receiver and transmitter coils were designed symmetrically. The location of the can to the side where the additional copper element (connecting ends of a coil) is present decreases the efficiency of WPT more noticeably than placement to the side where those are absent.

Chapter 6 - Conclusion and Future Work

The objective of this thesis was to model an inductive WPT system for underwater usage and perform a quantitative analysis of its behavior in different scenarios. This was conducted by testing the designed IPT in different media, namely in air, seawater, and more conductive water; testing in the presence of objects with different material types, sizes, thicknesses, and shapes; as well as testing the model when coils are not perfectly aligned.

The results suggest that the conductive environment causes more eddy current generation, decreasing the efficiency of WPT. Since the seawater exhibits electrical conductivity, it induces eddy currents at high frequencies. These eddy currents contribute to the rise of losses and impact the overall performance of the whole system. In this regard, the considerable decrease in the power transfer efficiency was observed with the increase in frequency in seawater environments.

The placement of foreign objects differently affects the system, depending on the induced eddy currents on them, the magnetization effect, and how localized the magnetic field is around the coil. The ferromagnetic metals caused an increase in inductance value due to the magnetization effect which reacts to the eddy currents. The effect of the latter one is dependent on the frequency however the former is independent of it. For non ferromagnetic metals, the magnetization is almost negligible, causing the inductance to drop below the reference point. The size of the metal plates do not considerably affect the performance of the system unless the dimensions exceed the geometry of the coil due to high localization of the magnetic field around it. The thickness of metal plates of all the studied materials improved the efficiency of underwater IPT since it locates the object in parallel with the main magnetic field. The circular plates tend to also increase the efficiency of the system rather than the rectangular ones, indicating the shape's influence on the underwater WPT system.

This work has explored some of the ferro and non ferromagnetic metal plates' effects on the performance of the underwater IPT system and it has demonstrated that any metal plate variable affects the system differently. The choice of interest for the material lay on pure metals only. In this regard, future work requires increasing the sample size of external object material, including common alloys of several pure metals, since the behavior of pure metals differs from that of their alloys. Due to the fact that many of foreign objects are generally composed of a mixture of different metals, this study would be beneficial in representing real-world case conditions.

Also, since the magnetic field density distribution plays a significant role in understanding the behavior of underwater IPT in the presence of foreign metal objects, future work includes studying the magnetic field distribution of the IPT system with and without an external object. The comparison between these two can give a deep insight into the reasoning behind such behavior of the wireless charging system.

To extend this work, the next scenario to investigate can be the placement of the foreign object near the receiver or transmitter, not between these resonators. Because such placements are also common, this will contribute to a study of foreign object influence on the performance of the underwater WPT system.

Finally, experimental validation of the performed simulation studies is required to identify the robustness of the results and their applicability in the real world.

Bibliography

[1] C. R. Teeneti, T. T. Truscott, D. N. Beal and Z. Pantic, "Review of Wireless Charging Systems for Autonomous Underwater Vehicles," in *IEEE Journal of Oceanic Engineering*, vol. 46, no. 1, pp. 68-87, Jan. 2021.

[2] A. M. Bradley, M. D. Feezor, H. Singh and F. Yates Sorrell, "Power systems for autonomous underwater vehicles," in *IEEE Journal of Oceanic Engineering*, vol. 26, no. 4, pp. 526-538, Oct. 2001.

[3] L. Yang et al., "Comparison Survey of Effects of Hull on AUVs for Underwater Capacitive Wireless Power Transfer System and Underwater Inductive Wireless Power Transfer System," in *IEEE Access*, vol. 10, pp. 125401-125410, 2022.

[4] R. Cox and S. Wei, "Advances in the state of the art for AUV inertial sensors and navigation systems," Proceedings of IEEE Symposium on Autonomous Underwater Vehicle Technology (AUV'94), Cambridge, MA, USA, 1994, pp. 360-369.

[5] T. Hyakudome, T. Nakatani, H. Yoshida, T. Tani, H. Ito and K. Sugihara, "Development of fuel cell system for long cruising lange Autonomous Underwater Vehicle," 2016 IEEE/OES Autonomous Underwater Vehicles (AUV), Tokyo, Japan, 2016, pp. 165-170.

[6] M. Lu, M. Bagheri, A. P. James and T. Phung, "Wireless Charging Techniques for UAVs: A Review, Reconceptualization, and Extension," in *IEEE Access*, vol. 6, pp. 29865-29884, 2018.

[7] J. M. Cena, “Power transfer efficiency of mutually coupled coils in an aluminum AUV hull,” M.S. thesis, Nav. Postgrad. School, Monterey, CA, USA, 2013.

[8] Z. Yan, K. Zhang, H. Wen, and B. Song, “Research on characteristics of contactless power transmission device for autonomous underwater vehicle,” in Proc. OCEANS Conf., 2016, pp. 1–5.

[9] W. Haibing, Z. Kehan, Y. Zhengchao, and S. Baowei, “Comparison of two electromagnetic couplers in an inductive power transfer system for autonomous underwater vehicle docking application,” in Proc. OCEANS Conf., 2016, pp. 1–5.

[10] D. Wang, S. Cui, J. Zhang, Z. Bie, K. Song and C. Zhu, "A Novel Arc-Shaped Lightweight Magnetic Coupler for AUV Wireless Power Transfer," in IEEE Transactions on Industry Applications, vol. 58, no. 1, pp. 1315-1329, Jan.-Feb. 2022.

[11] W. Xiao, R. Shen, B. Zhang, D. Qiu, Y. Chen and T. Li, "Effect of Foreign Metal Object on Soft-Switching Conditions of Class-E Inverter in WPT," Energies, vol. 11, no. 1926, pp. 1-19, 2018.

[12] B. J. B. Deutschmann, L. Görtschacher, P. Priller and J. Grosinger, "Efficient Assessment of the Impact of Metallic Obstacles on the Wireless Power Transfer in Loosely Coupled Links," 2019 49th European Microwave Conference (EuMC), Paris, France, 2019, pp. 579-582.

[13] S. Y. Jeong, H. G. Kwak, G. C. Jang, S. Y. Choi and C. T. Rim, "Dual-Purpose Nonoverlapping Coil Sets as Metal Object and Vehicle Position Detections for Wireless Stationary EV Chargers," in IEEE Transactions on Power Electronics, vol. 33, no. 9, pp. 7387-7397, Sept. 2018.

[14] J. Xiao, H. Shi, S. Chen, X. Wu, W. Gong and Y. Mo, "Research on Self-powering Technology of Foreign Object Detection Circuit in Wireless Power Transfer System," 2023 International Conference on Computers, Information Processing and Advanced Education (CIPAE), Ottawa, ON, Canada, 2023, pp. 1-7.

[15] S. Son et al., "Foreign Object Detection of Wireless Power Transfer System Using Sensor Coil," 2021 IEEE Wireless Power Transfer Conference (WPTC), San Diego, CA, USA, 2021, pp. 1-4.

[16] S. S. H. Yazdi, S. Shafiei, A. Kapanov, Y. Shakhin, A. Namadmalan and M. Bagheri, "Enhanced Domino Wireless Power Transfer for Transmission Line Monitoring: Overcoming External Metal Object Interference and Optimizing Coil Design," in IEEE Transactions on Power Delivery, vol. 39, no. 2, pp. 1137-1150, April 2024.

[17] A. Smagulova and M. Bagheri, "Low Frequency Domino Wireless Power Transfer: A Simulation Study and Analysis," 2020 9th International Conference on Renewable Energy Research and Application (ICRERA), Glasgow, UK, 2020, pp. 196-201.

[18] L. Yang, L. Ma, J. Huang and Y. Fu, "Characteristics of Undersea Capacitive Wireless Power Transfer System," *2020 IEEE 9th International Power Electronics and Motion Control Conference (IPEMC2020-ECCE Asia)*, Nanjing, China, 2020, pp. 2952-2955.

[19] S. Y. R. Hui, "Past, present and future trends of non-radiative wireless power transfer," in *CPSS Transactions on Power Electronics and Applications*, vol. 1, no. 1, pp. 83-91, Dec. 2016.

[20] S. Shafiei, S. S. Heidari Yazdi, T. Mussin, Y. Shakhin, A. Namadmalan and M. Bagheri, "Analyzing the Impacts of High Voltage Insulators on Equivalent Parameters of Wireless Power Transfer: Simulation and Experimental Studies," 2022 IEEE Electrical Power and Energy Conference (EPEC), Victoria, BC, Canada, 2022, pp. 424-429.

[21] A. Rakhymbay, M. Bagheri and M. Lu, "A simulation study on four different compensation topologies in EV wireless charging," 2017 International Conference on Sustainable Energy Engineering and Application (ICSEEA), Jakarta, Indonesia, 2017, pp. 66-73.

[22] T. Kojiya, F. Sato, H. Matsuki, and T. Sato, “Construction of noncontacting power feeding system to underwater vehicle utilizing electro magnetic induction,” in *Proc. Eur. OCEANS Conf*., 2005, vol. 1, pp. 709–712.

[23] B. J. Heeres, D. W. Novotny, D. M. Divan, and R. D. Lorenz, “Contactless underwater power delivery,” in *25th Annu. IEEE Power Electron. Spec. Conf. Rec.*, 1994, pp. 418–423.

[24] M. D. Feezor, F. Yates Sorrell, and P. R. Blankinship, “An interface system for autonomous undersea vehicles,” *IEEE J. Ocean. Eng*., vol. 26, no. 4, pp. 522–525, Oct. 2001.

[25] S. Shafiei, S. S. H. Yazdi, M. Kermani, A. Saukhimov, A. Hekmati and M. Bagheri, "Underwater and In-Air IPT-CPT Wireless Power Transfer Performance Comparison: A Simulation Study," *2023 IEEE International Conference on Environment and Electrical Engineering and 2023 IEEE Industrial and Commercial Power Systems Europe (EEEIC / I&CPS Europe)*, Madrid, Spain, 2023, pp. 1-6.

[26] T. Kojiya, F. Sato, H. Matsuki, and T. Sato, “Automatic power supply system to underwater vehicles utilizing non-contacting technology,” in Proc. Oceans MTTS/IEEE Techno-Ocean, Nov. 2004, vol. 4, pp. 2341– 2345.

[27] M. N. O. Sadiku, Elements of Electromagnetics, Oxford: Oxford University Press, 2010.

[28] D. Vincent, P. S. Huynh, N. A. Azeez, L. Patnaik and S. S. Williamson, "Evolution of Hybrid Inductive and Capacitive AC Links for Wireless EV Charging—A Comparative Overview," in IEEE Transactions on Transportation Electrification, vol. 5, no. 4, pp. 1060-1077, Dec. 2019.

[29] F. Lu, H. Zhang, H. Hofmann and C. C. Mi, "An Inductive and Capacitive Combined Wireless Power Transfer System With LC-Compensated Topology," in IEEE Transactions on Power Electronics, vol. 31, no. 12, pp. 8471-8482, Dec. 2016.

[30] T. Kan, Y. Zhang, Z. Yan, P. P. Mercier and C. C. Mi, "A Rotation-Resilient Wireless Charging System for Lightweight Autonomous Underwater Vehicles," in IEEE Transactions on Vehicular Technology, vol. 67, no. 8, pp. 6935-6942, Aug. 2018.

[31] Z. Yan, B. Song, Y. Zhang, K. Zhang, Z. Mao and Y. Hu, "A Rotation-Free Wireless Power Transfer System With Stable Output Power and Efficiency for Autonomous Underwater Vehicles," in IEEE Transactions on Power Electronics, vol. 34, no. 5, pp. 4005-4008, May 2019.

[32] Yan, Z.; Song, B.; Zhang, K.; Wen, H.; Mao, Z.; Hu, Y., “Eddy CurrentLoss Analysis of Underwater Wireless Power Transfer Systems withMisalignments,”AIP Adv., vol. 8, pp. 101421, 2018

[33] Yan, Zhengchao, et al. "Underwater wireless power transfer system with a curly coil structure for AUVs." IET Power Electronics 12.10 (2019): 2559-2565.

[34] J. Hu, X. Meng, Y. Ma, Z. Chu and Y. Wang, "Analysis and Comparison of Underwater Wireless Charging System Topology," 2023 IEEE 6th International Conference on Automation, Electronics and Electrical Engineering (AUTEEE), Shenyang, China, 2023, pp. 100-105.

[35] Y. Xu, J. Yang, M. Zeng and L. Dong, "Wireless Power Transfer System of AUV Based on Improved Coil Structure With Stable Output Power and Efficiency," 2022 IEEE 17th Conference on Industrial Electronics and Applications (ICIEA), Chengdu, China, 2022, pp. 561-565.

[36] A. Smagulova, S. S. H. Yazdi and M. Bagheri, "Design, Simulation, and Comparison of Wireless Power Transfer Systems with Single and Multiple Resonator Coils for UAVs," *2021 10th International Conference on Renewable Energy Research and Application (ICRERA)*, Istanbul, Turkey, 2021, pp. 344-350.

[37] S. S. H. Yazdi et al., "A Wireless Charging System Based on a DR-IPT to Power a UAV From Distribution Poles," in IEEE Transactions on Industry Applications, vol. 59, no. 6, pp. 7757-7770, Nov.-Dec. 2023.

[38] J. Kim, K. Kim, H. Kim, D. Kim, J. Park and S. Ahn, "An Efficient Modeling for Underwater Wireless Power Transfer Using Z-Parameters," in IEEE Transactions on Electromagnetic Compatibility, vol. 61, no. 6, pp. 2006-2014, Dec. 2019.

[39] M. Tamura, Y. Naka, K. Murai, and T. Nakata, ‘‘Design of a capacitive wireless power transfer system for operation in fresh water,’’ *IEEE Trans. Microw. Theory Techn.*, vol. 66, no. 12, pp. 5873–5884, Dec. 2018.

[40] S. S. Biswal, D. P. Kar and S. Bhuyan, "Consideration of Series-Series and Series-Parallel Topology in Perspective of Dynamic Resonant Inductive Coupling Based Wireless Charging," 2021 1st Odisha International Conference on Electrical Power

Engineering, Communication and Computing Technology(ODICON), Bhubaneswar, India, 2021, pp. 1-4.

[41] W. Wenbin et al., "Modeling and Control Strategy for Zero Voltage Switching Condition in Series-Series Compensated Inductive Power Transfer System," 2019 14th IEEE Conference on Industrial Electronics and Applications (ICIEA), Xi'an, China, 2019, pp. 713-717.

[42] M. Singh, S. Samanta and S. P. Das, "A Generalized Method of Determining Coil and Compensation Circuit Parameters of Basic WPT Topologies," 2021 National Power Electronics Conference (NPEC), Bhubaneswar, India, 2021, pp. 1-6.

[43] M. T. Haque, A. A. Mohaimen and M. A. Arafat, "Analysis of Coupling Coefficient and Source Frequency Variations in Basic Compensation Topologies of MRC Based WPT Systems," 2022 12th International Conference on Electrical and Computer Engineering (ICECE), Dhaka, Bangladesh, 2022, pp. 308-311.

[44] Y. Dou, D. Zhao, Z. Ouyang and M. A. E. Andersen, "Investigation and Design of Wireless Power Transfer System for Autonomous Underwater Vehicle," 2019 IEEE Applied Power Electronics Conference and Exposition (APEC), Anaheim, CA, USA, 2019, pp. 3144-3150.

[45] A. Sagar et al., "A Comprehensive Review of the Recent Development of Wireless Power Transfer Technologies for Electric Vehicle Charging Systems," in IEEE Access, vol. 11, pp. 83703-83751, 2023.

[46] W. Zhang and C. C. Mi, “Compensation topologies of high-power wire- less power transfer systems,” IEEE Transactions on Vehicular Technology, vol. 65, no. 6, pp. 4768–4778, jun 2016.

[47] J. Henry, "Eddy Currents," Princeton University, [Online]. Available: http://www.princeton.edu/ssp/joseph-henry-project/eddy- currents/eddy_wiki.pdf. [Accessed: 9 March 2024].

[48] T. M. Hayslett, T. Orekan and P. Zhang, "Underwater wireless power transfer for ocean system applications," OCEANS 2016 MTS/IEEE Monterey, Monterey, CA, USA, 2016, pp. 1-6.